



Electromagnetic Scattering from Arbitrary Bodies Using Rao-Wilton-Glisson (RWG) Functions

Sadasiva M. Rao
Code # 5314
Radar Division
Naval Research Laboratory
Washington D.C. 20375 (USA)



Arbitrarily-Shaped Body

- Arbitrary shape.
- Arbitrary material composition.
- Cavities, cables, and apertures.
- Single or multiple bodies.
- Intersecting surfaces.
- Periodic structures.
- Finite structures.

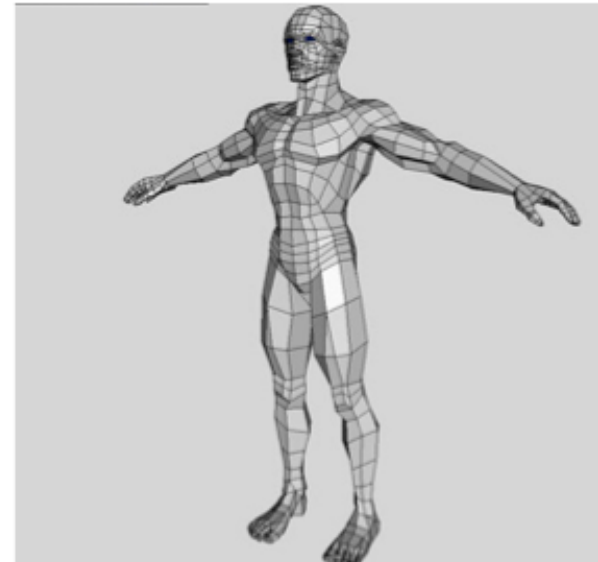
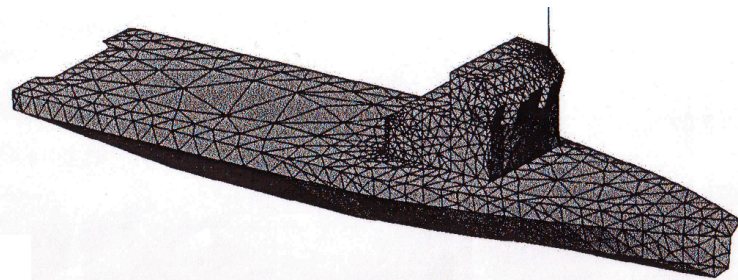
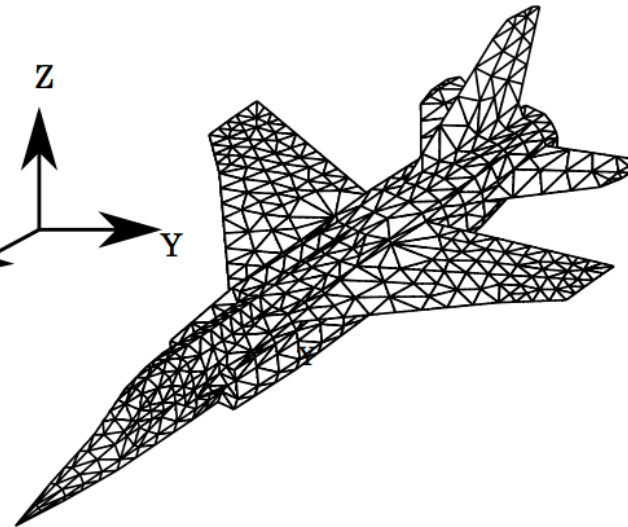
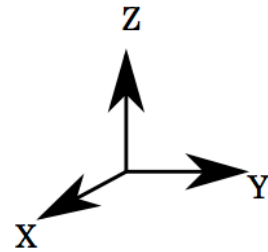
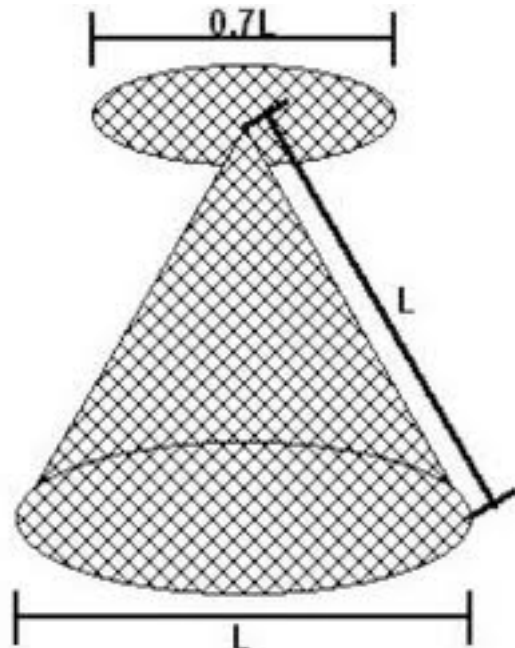


Numerical Solution Procedure

1. Describe Geometry to the computer- Planar triangular patch modeling.
2. Transform the Mathematical Equations into Matrix equation via Method of Moments.
3. Solve the Matrix equation.
4. Post-processing.



Triangulated Models





Method of Moments Solution

$$AX = Y \quad (4)$$

$$X = \sum_{i=1}^N \alpha_i p_i \quad (5)$$

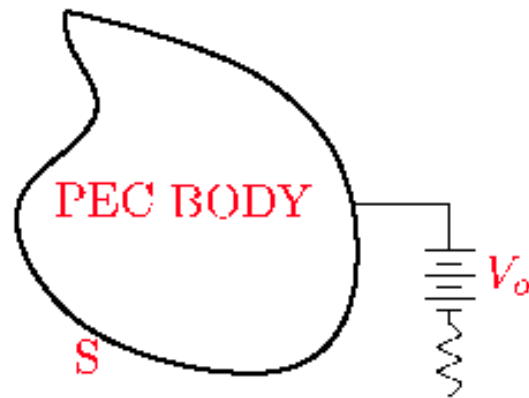
$$\sum_{i=1}^N \alpha_i A p_i = Y \quad (6)$$

$$\sum_{i=1}^N \alpha_i \langle q_j, A p_i \rangle = \langle q_j, Y \rangle \quad j = 1, 2, \dots, N \quad (7)$$

$$\Rightarrow ZX = Y \quad (8)$$



Electrostatic Problems



Applications: Electrostatic Discharge (ESD)

Method: Calculate charge distribution

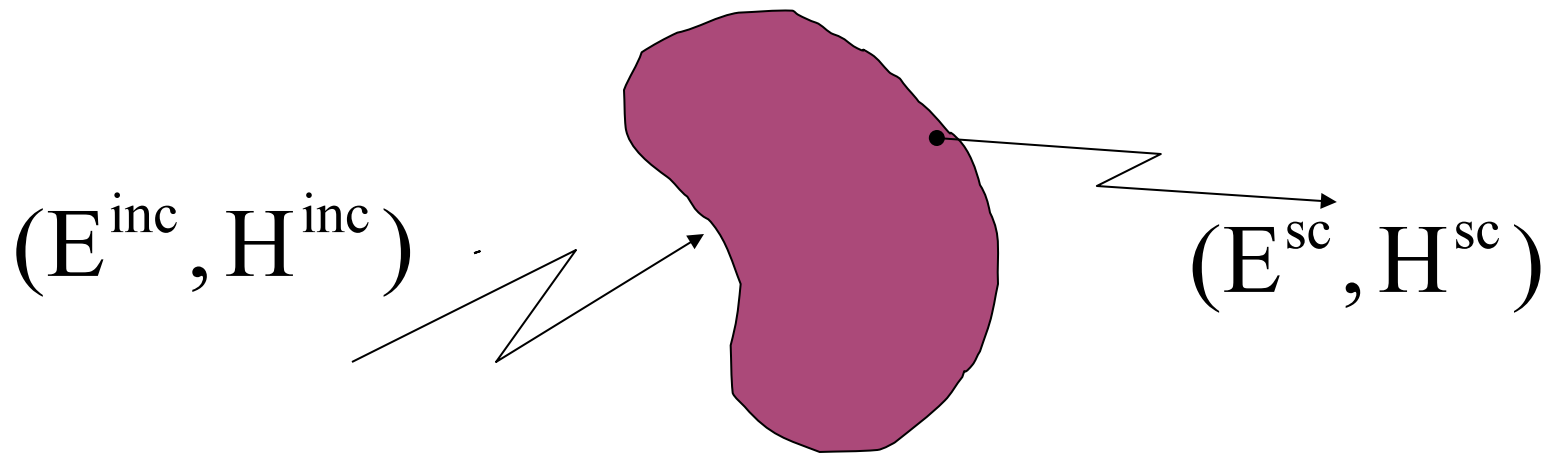
$$\int_S \frac{q_s(\mathbf{r}')}{|\mathbf{r} - \mathbf{r}'|} dS' = 4\pi\epsilon_0 V_o \quad \text{rc}S$$
$$\Rightarrow \sum_{i=1}^N Q_i \int_{T_i} \frac{dS'}{|\mathbf{r}_j^c - \mathbf{r}'|} = 4\pi\epsilon_0 V_{o_j}$$
$$j = 1, 2, \dots, N$$
$$\Rightarrow [Z][Q] = [V]$$



-
- Charge calculation – IEEE Trans. A&P 1979
 - Electrostatic Discharge on Multi-Conductor Transmission Lines – IEEE Trans. MTT 1984
 - Power-line hazard analysis - IEEE Trans. MTT 1985
 - Characterization of Cross talk problem in VLSI design - IEEE Trans. MTT 1998
 - Nuclear EMP Studies



Electrodynamics Problems



Arbitrary PEC Body excited by a Plane wave

EFIE

$$\begin{aligned}\mathbf{E}_{tan}^{total} &= 0 \text{ for } \mathbf{r} \in S \\ \Rightarrow \mathbf{E}_{tan}^{inc} + \mathbf{E}_{tan}^{sc} &= 0 \\ \Rightarrow [j\omega\mathbf{A} + \nabla\Phi]_{tan} &= \mathbf{E}_{tan}^{inc} \text{ for } \mathbf{r} \in S\end{aligned}$$

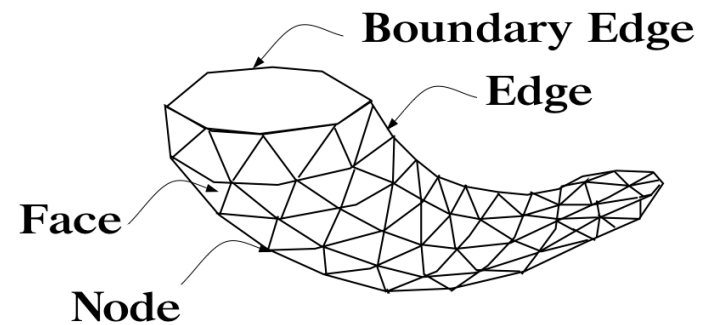
MFIE

$$\begin{aligned}\mathbf{J} &= \mathbf{a}_n \times \mathbf{H}^{total} \text{ for } \mathbf{r} \in S \\ \Rightarrow \mathbf{J} &= \mathbf{a}_n \times (\mathbf{H}^{inc} + \mathbf{H}^{sc}) \\ \Rightarrow \mathbf{J} - \mathbf{a}_n \times \mathbf{H}^{sc} &= \mathbf{a}_n \times \mathbf{H}^{inc} \text{ for } \mathbf{r} \in S\end{aligned}$$



Method of Moments Solution Procedure

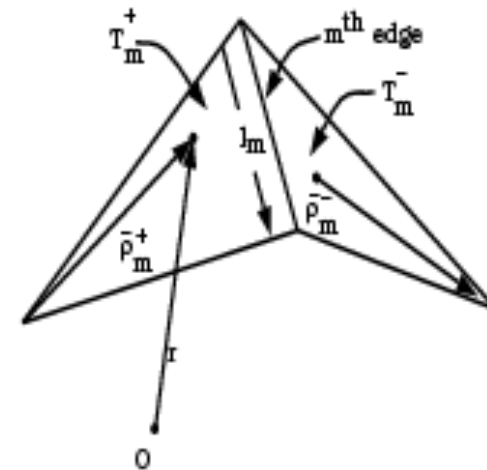
Approximate the unknown current density using RWG (Rao-Wilton-Glisson) functions.



Triangulated Body

$$\underline{\mathbf{J}} = \sum I_n \underline{\mathbf{f}}_n$$

$$\underline{\mathbf{f}}_n = \begin{cases} \frac{l_n}{2\mathbf{A}_n^+} \rho_n^+ & \mathbf{r} \in \mathbf{T}_n^+ \\ \frac{l_n}{2\mathbf{A}_n^-} \rho_n^- & \mathbf{r} \in \mathbf{T}_n^- \\ \mathbf{0} & \text{otherwise} \end{cases}$$

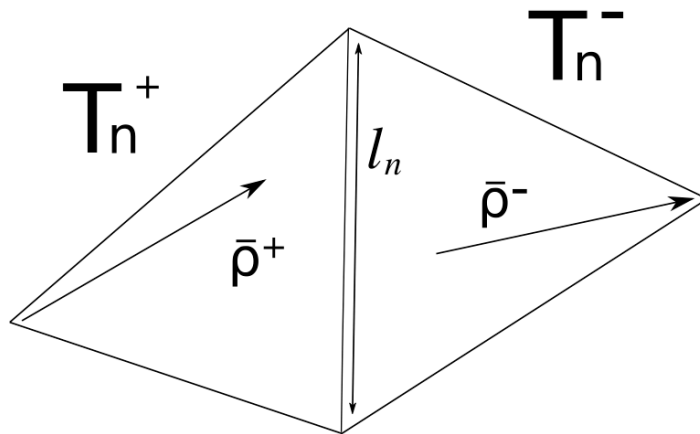


RWG Basis functions



Method of Moments Solution Procedure

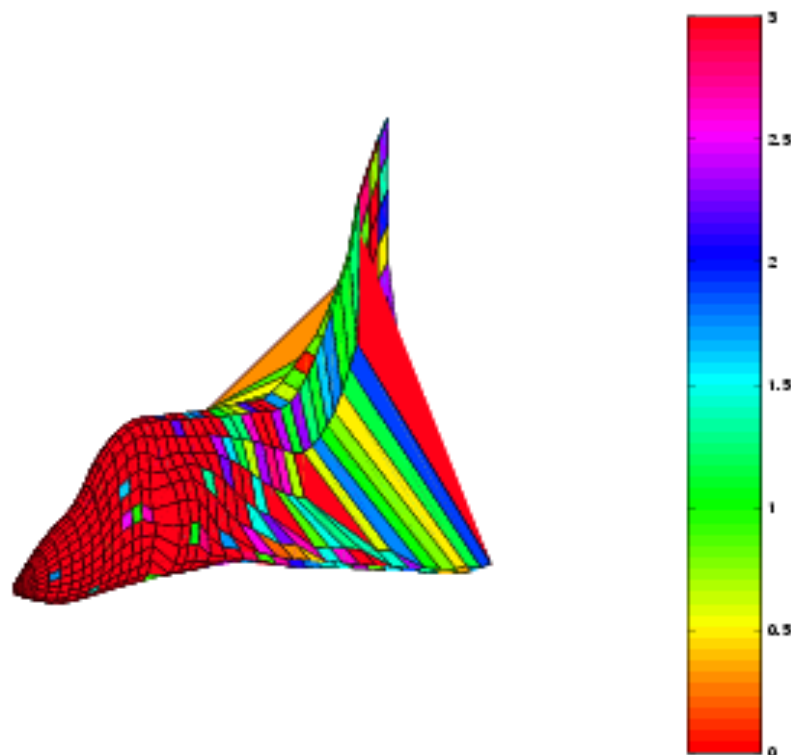
- Transform the operator equation into matrix equation using testing functions – Also RWG functions.
- Solve the matrix equation.



Testing Functions



Example of the currents on an Aircraft at 300 MHz with 2900 unknowns





Base Station Antenna Design

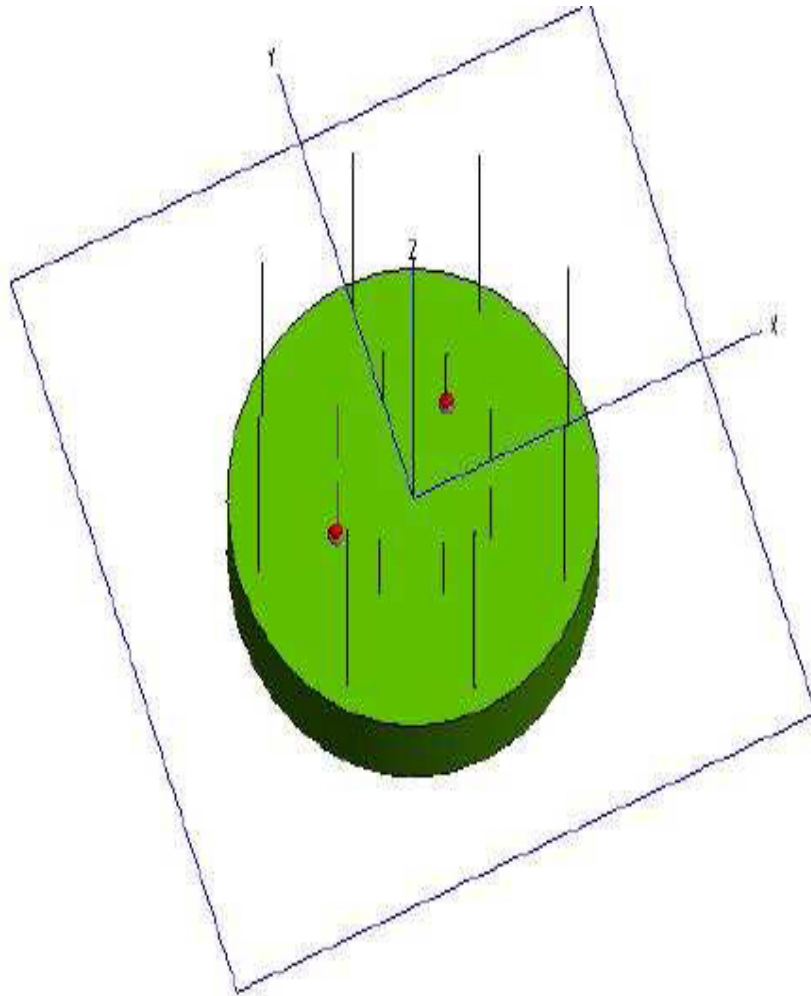


Figure: Geometry of the array antenna

- 1 element placed at the center of the cylindrical ground plane.
- 16 elements distributed uniformly (45° apart) on the circumference of 2 concentric rings.
- Two driver elements shown with red ports.
- 17 elements in all.



Geometry of antenna

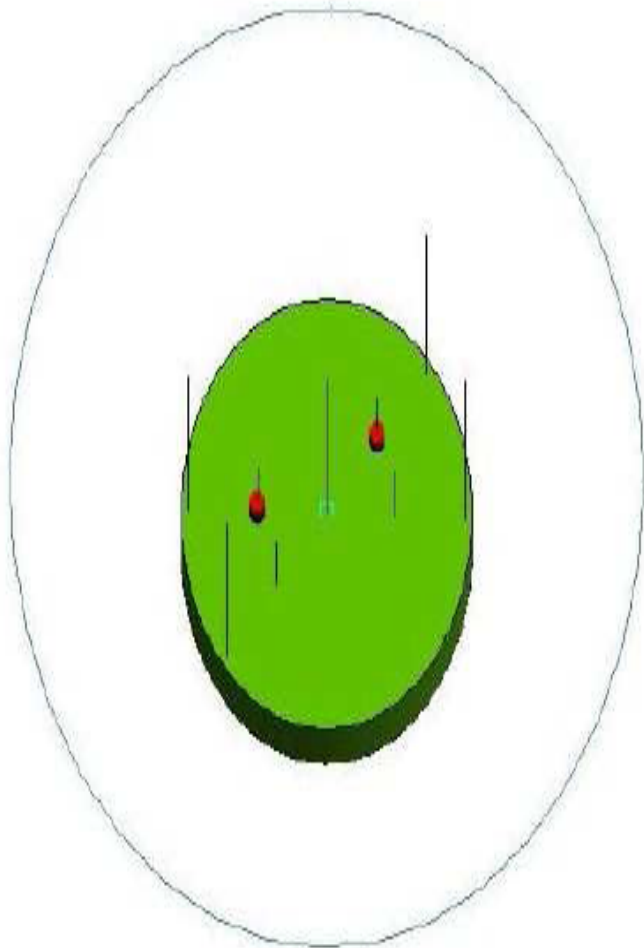
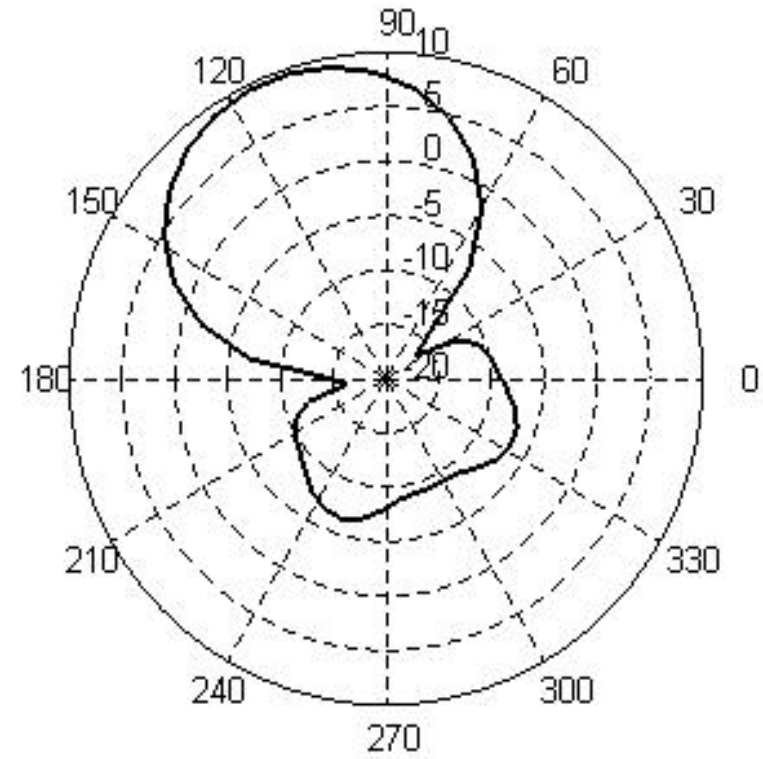
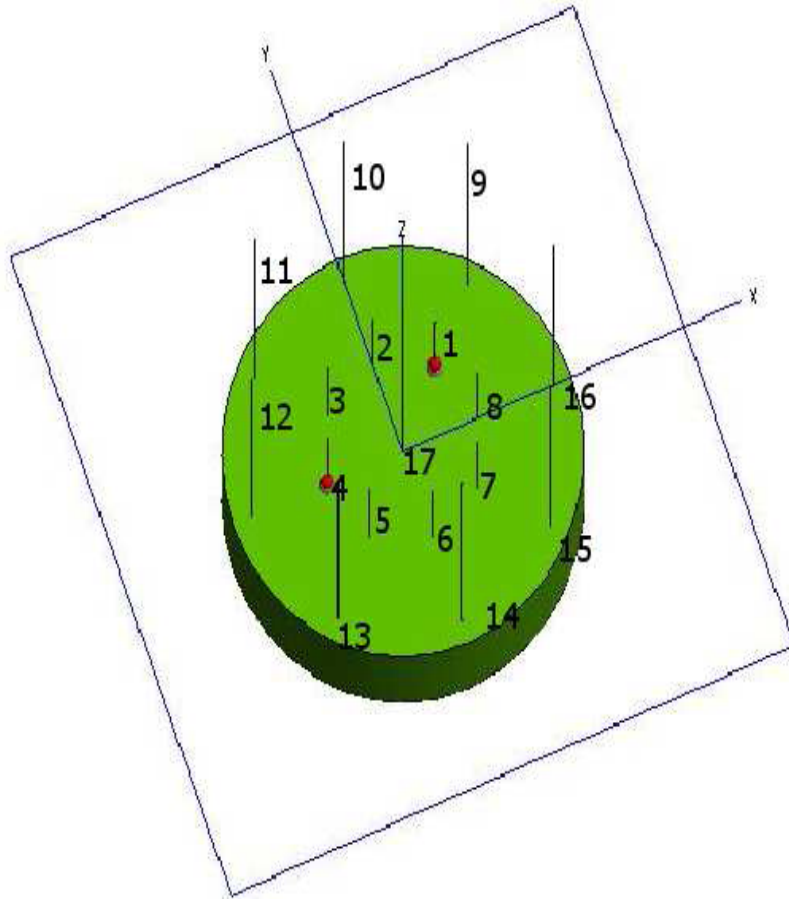


Figure : Geometry of the antenna with only essential elements.

- 9 elements
- Driver elements are present in the inner circle and they are 135° apart.
- The elements in inner circle act as directors.
- Elements in the outer circle act as reflectors.
- Hollow cylinder acts as ground plane.

Far Field Gain in Horizontal Plane

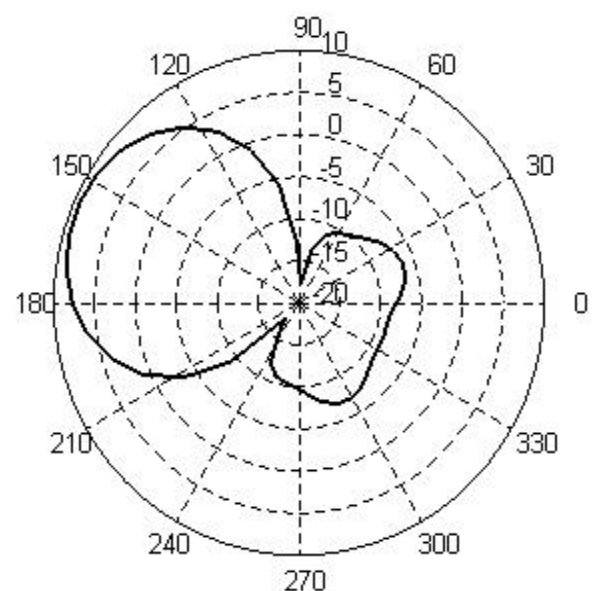
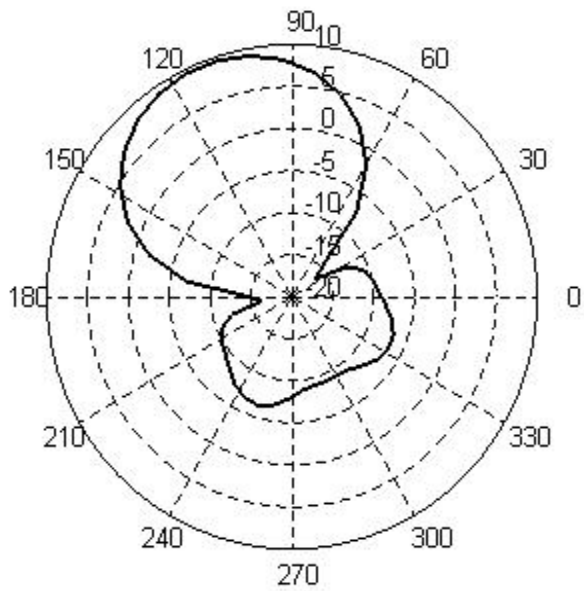
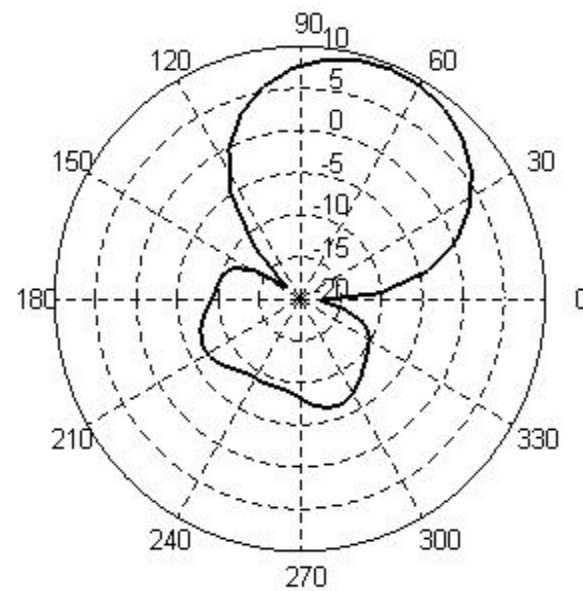
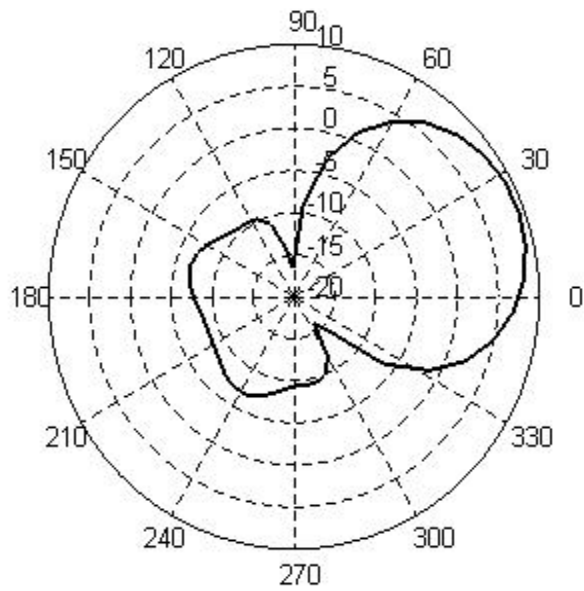


Angle (Phi, Degrees)

Elements 1 and 4 are excited
8, 16, 17, 12, 9, 5, 13 are grounded
and the remaining elements are removed from the system.
(open circuited)

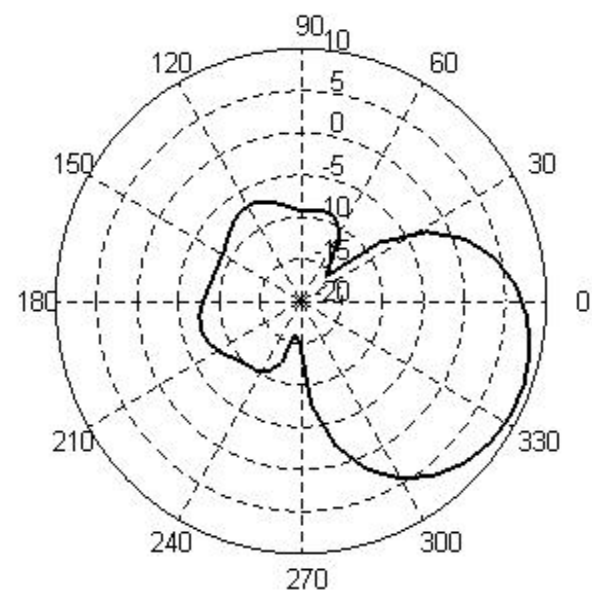
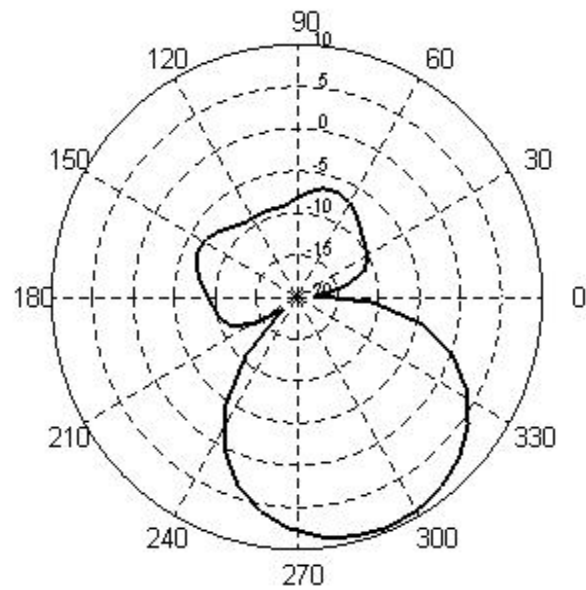
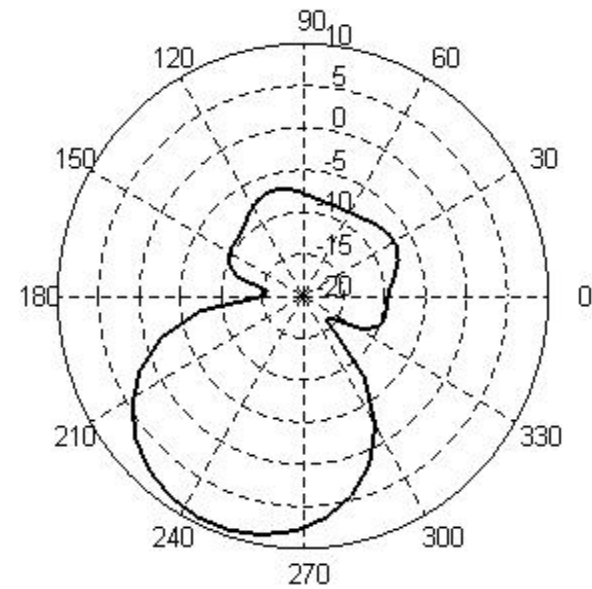
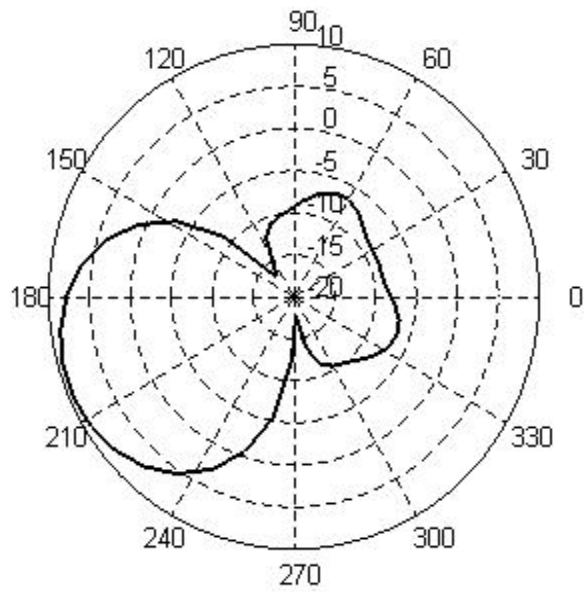


Far Field Gain in Horizontal Plane





Far Field Gain in Horizontal Plane





Fabrication of Antenna

- The antenna was fabricated to operate at 2GHz frequency.
- Copper sheets and rods of optimized dimensions were used for construction.
- A power splitter was designed to split the power equally between two driver elements.



Figure: Top view of the fabricated antenna



Fabricated antenna

- $h_c = 1.1811$ inches (Height of the cylindrical ground plane)
- $r_c = 3.3070$ inches (Radius of the cylindrical ground plane)
- $h_i = 1.5029$ inches (Height of elements on inner circle)
- $h_o = 4.7238$ inches (Height of elements on outer circle)
- $h_{org} = 4.7096$ inches (Height of element at origin)
- $r_i = 1.5750$ inches (Radius of inner circle)
- $r_o = 3.1500$ inches (Radius of outer circle)
- $r_r = 0.0625$ inches (Radius of antenna elements)

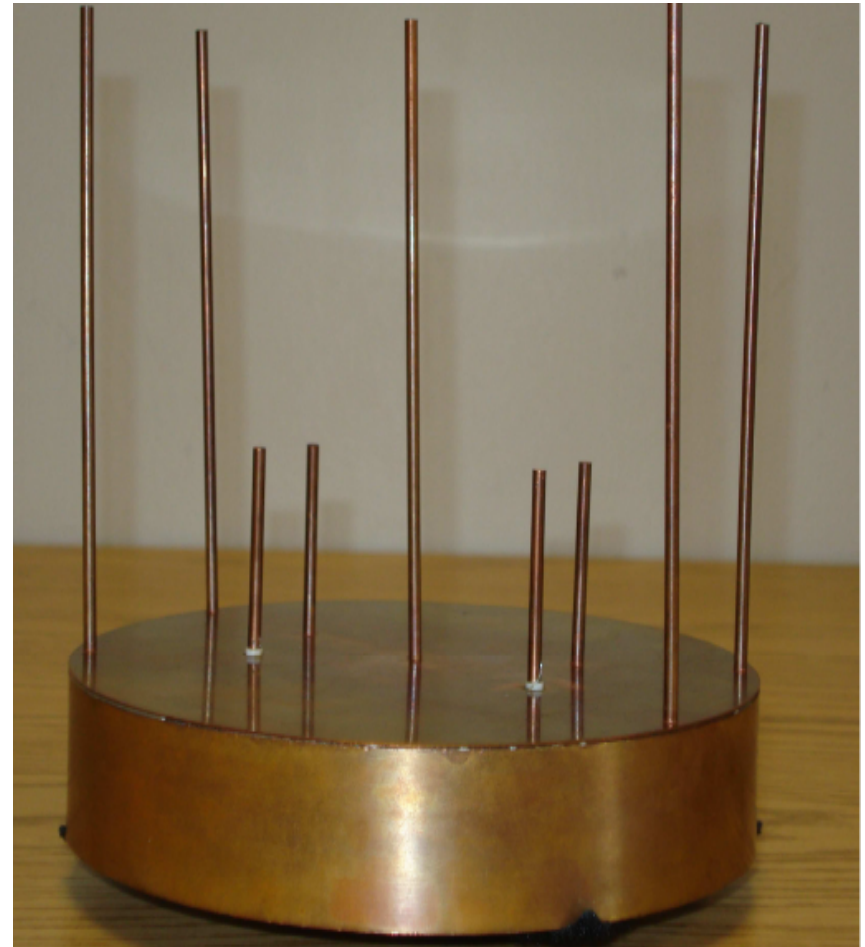


Figure: Side view of fabricated antenna



Comparison of the Radiation Patterns

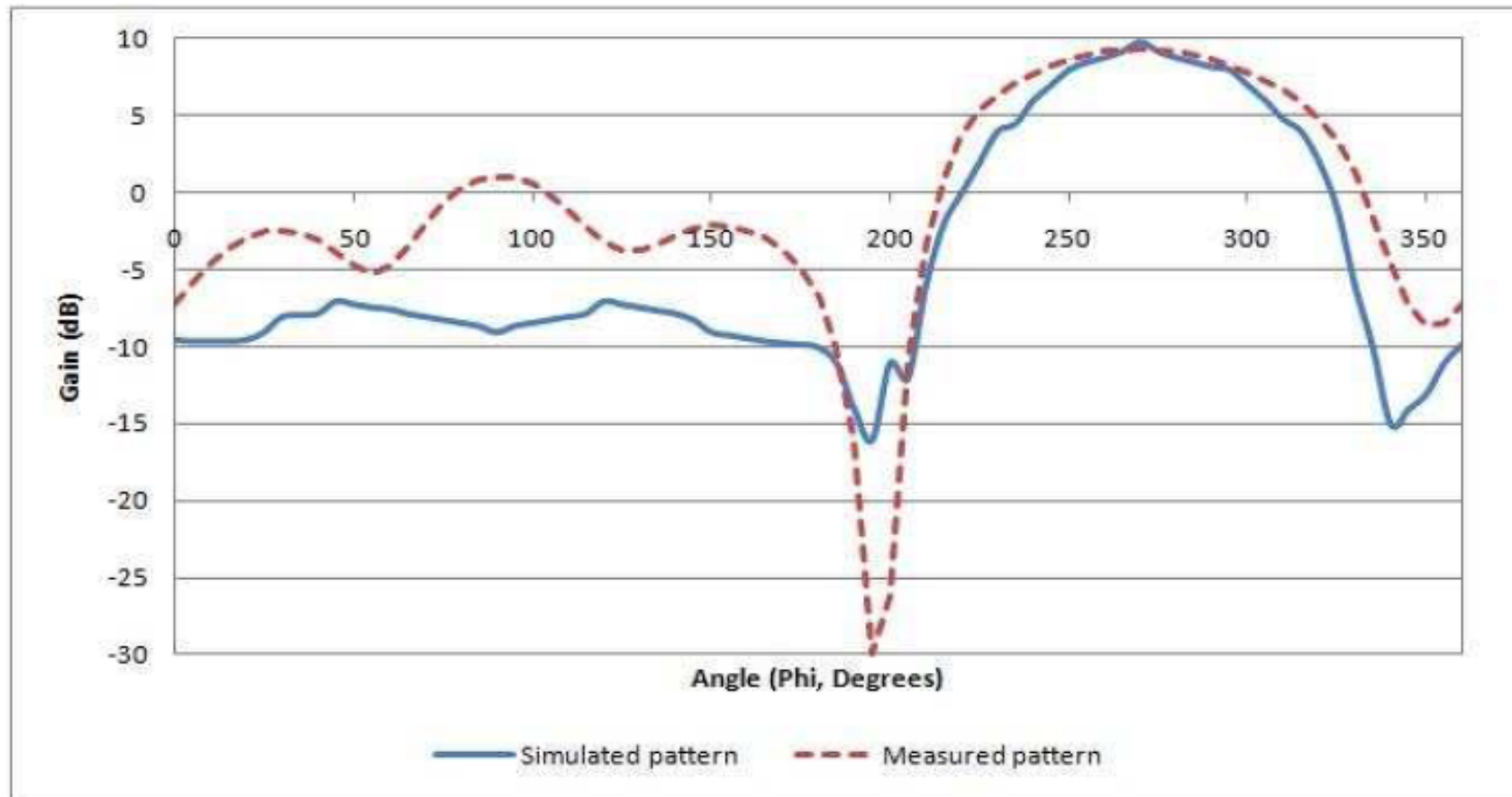


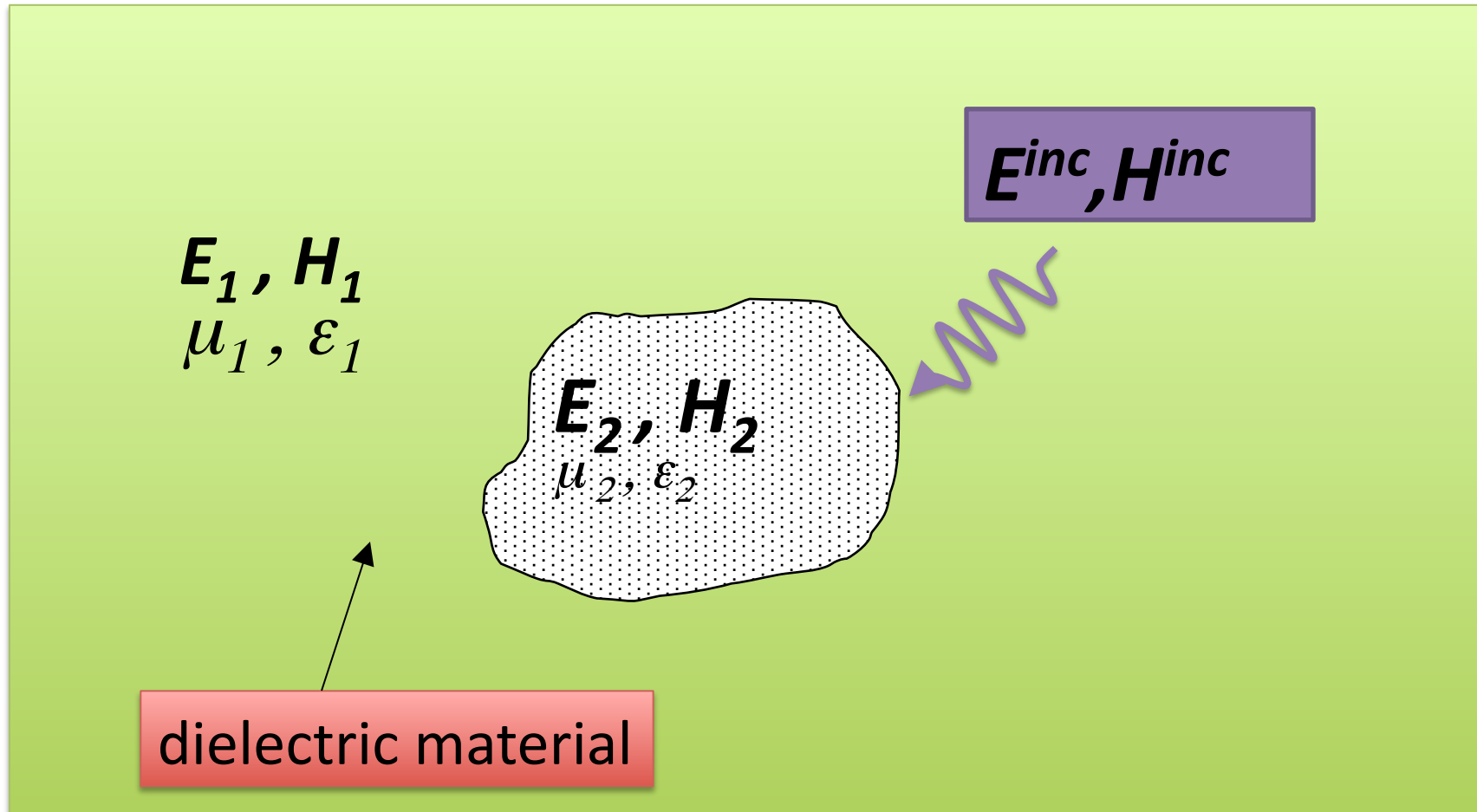
Figure: The simulated and measured radiation patterns of antenna



-
- FERM – Lincoln Labs – This code is classified
 - PATCH – Sandia National Labs – This code is classified
 - IE3D – Commercial Code
 - FEKO – Commercial Code
 - CARLOS3D – McDonnell Douglas

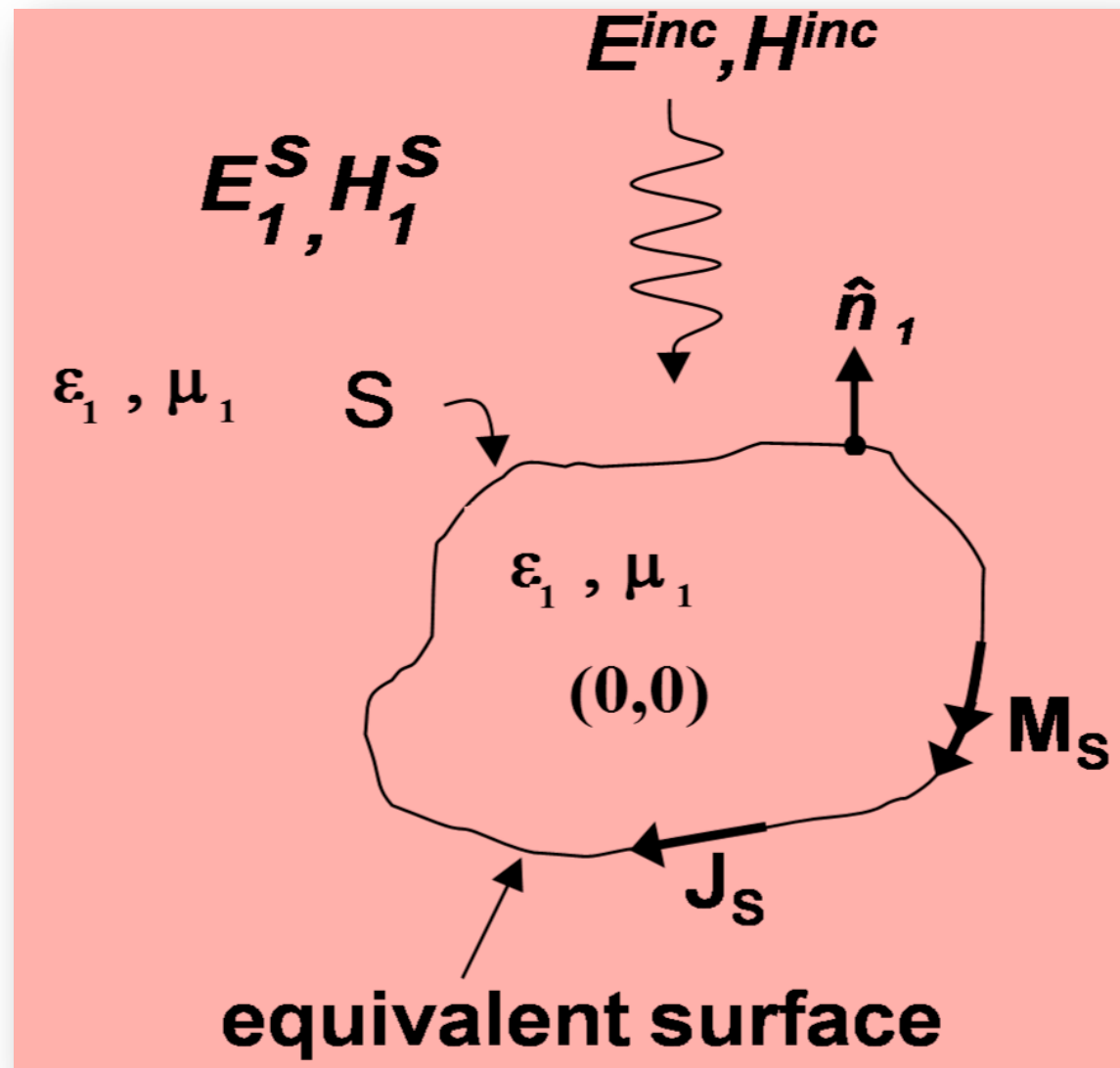


Surface Formulation of Integral Equations For a Dielectric Body



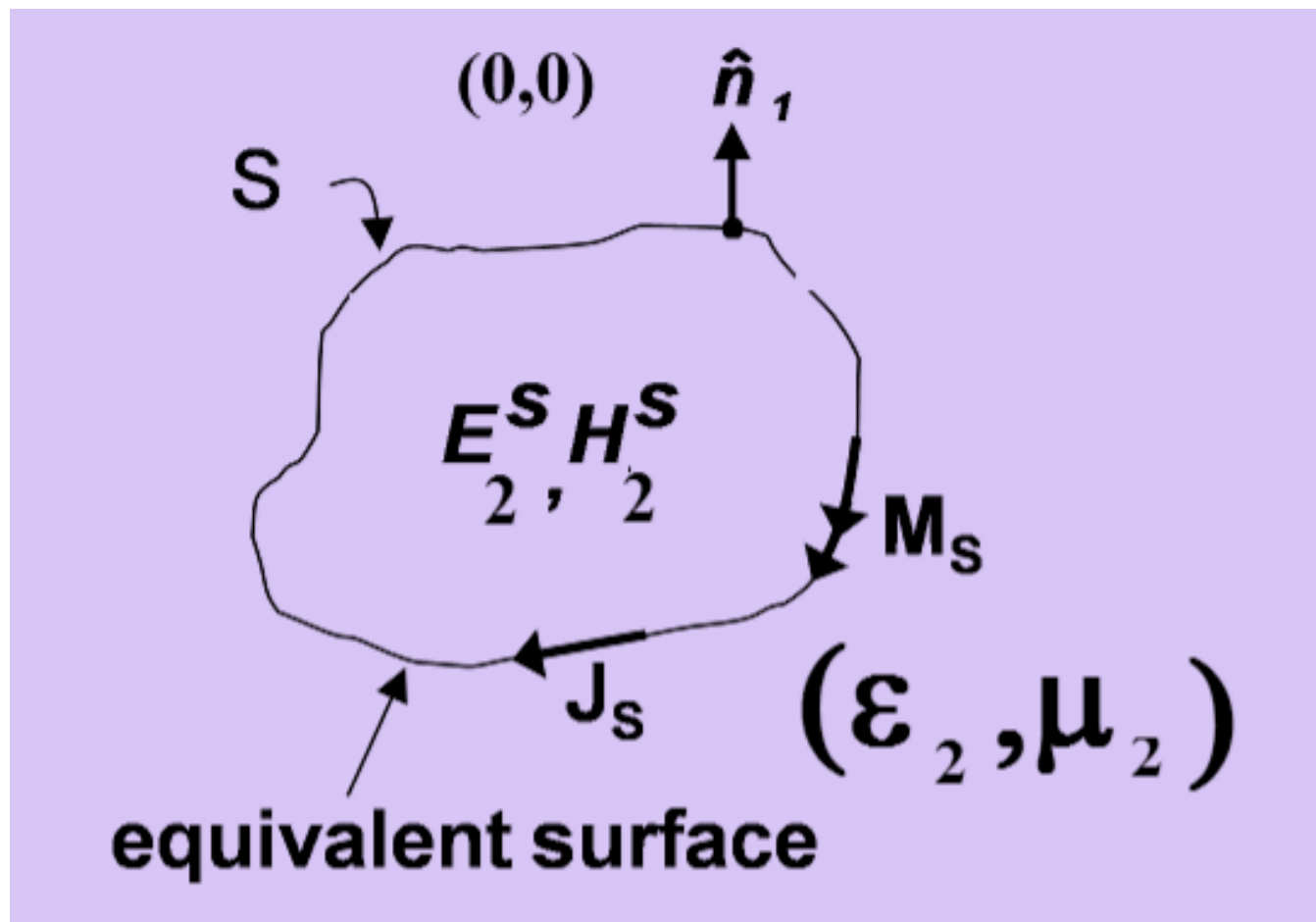


External Equivalent Problem





Internal Equivalent Problem





Four Governing Equations

$$\begin{aligned} [\mathbf{E}_1^s(\mathbf{J}_s) + \mathbf{E}_1^s(\mathbf{M}_s) + \mathbf{E}^{inc}]_{tan} &= 0 \text{ for } \mathbf{r} \in S \\ [\mathbf{H}_1^s(\mathbf{J}_s) + \mathbf{H}_1^s(\mathbf{M}_s) + \mathbf{H}^{inc}]_{tan} &= 0 \text{ for } \mathbf{r} \in S \end{aligned}$$

$$\begin{aligned} [\mathbf{E}_2^s(\mathbf{J}_s) + \mathbf{E}_2^s(\mathbf{M}_s)]_{tan} &= 0 \text{ for } \mathbf{r} \in S \\ [\mathbf{H}_2^s(\mathbf{J}_s) + \mathbf{H}_2^s(\mathbf{M}_s)]_{tan} &= 0 \text{ for } \mathbf{r} \in S \end{aligned}$$

Where

$$\begin{aligned} \mathbf{E}_{1,2}^s(\mathbf{J}_s) &= j\omega \mathbf{A}_{1,2} + \nabla \Phi_{1,2} \\ \mathbf{E}_{1,2}^s(\mathbf{M}_s) &= \pm \mathbf{a}_n \times \frac{\mathbf{M}_s}{2} + \nabla \times \mathbf{F}_{1,2} \\ \mathbf{H}_{1,2}^s(\mathbf{M}_s) &= j\omega \mathbf{F}_{1,2} + \nabla \Psi_{1,2} \\ \mathbf{H}_{1,2}^s(\mathbf{J}_s) &= \mp \mathbf{a}_n \times \frac{\mathbf{J}_s}{2} + \nabla \times \mathbf{A}_{1,2} \end{aligned}$$



SIE Formulations

- PMCHWT Formulation
- EFIE Formulation
- MFIE Formulation
- CFIE Formulation
- Muller Formulation



PMCHWT Formulation

$$\begin{aligned} [\mathbf{E}_1^s + \mathbf{E}_2^s]_{tan} &= -\mathbf{E}_{tan}^{inc} \quad \text{for } \mathbf{r} \in S \\ [\mathbf{H}_1^s + \mathbf{H}_2^s]_{tan} &= -\mathbf{H}_{tan}^{inc} \quad \text{for } \mathbf{r} \in S \end{aligned}$$

Resulting in

$$\begin{aligned} [j\omega (\mathbf{A}_1 + \mathbf{A}_2) + \nabla (\Phi_1 + \Phi_2) + \nabla \times (\mathbf{F}_1 + \mathbf{F}_2)]_{tan} &= \mathbf{E}_{tan}^{inc} \\ [-\nabla \times (\mathbf{A}_1 + \mathbf{A}_2) + j\omega (\mathbf{F}_1 + \mathbf{F}_2) + \nabla (\Psi_1 + \Psi_2)]_{tan} &= \mathbf{H}_{tan}^{inc} \end{aligned}$$

- ◆ Expansion Procedure – Use RWG Functions for both \mathbf{J}_s and \mathbf{M}_s .
- ◆ Testing Procedure – Use RWG Functions - similar to PEC Case.
- ◆ Most Efficient Solution – Acceptable accuracy.
- ◆ However, the same procedure fails for other formulations – Why?



EFIE Formulation

$$[\mathbf{E}_1^s(\mathbf{J}_s) + \mathbf{E}_1^s(\mathbf{M}_s)]_{tan} = -\mathbf{E}_{tan}^{inc} \text{ for } \mathbf{r} \in S$$

$$[\mathbf{E}_2^s(\mathbf{J}_s) + \mathbf{E}_2^s(\mathbf{M}_s)]_{tan} = 0 \text{ for } \mathbf{r} \in S$$

Resulting in

$$\left[j\omega \mathbf{A}_1 + \nabla \Phi_1 + \mathbf{a}_n \times \frac{\mathbf{M}_s}{2} + \nabla \times \mathbf{F}_1 \right]_{tan} = \mathbf{E}_{tan}^{inc}$$
$$\left[j\omega \mathbf{A}_2 + \nabla \Phi_2 - \mathbf{a}_n \times \frac{\mathbf{M}_s}{2} + \nabla \times \mathbf{F}_2 \right]_{tan} = 0$$

- ◆ Expansion Procedure – Let us assume RWG Functions for both \mathbf{J}_s and \mathbf{M}_s .
- ◆ Testing Procedure – Use RWG Functions

◆ What happens?



RWG Testing functions

$$\begin{pmatrix} \mathbf{Z}_E^1(\mathbf{J}_s) & \mathbf{Z}_E^1(\mathbf{M}_s) \\ \mathbf{Z}_E^2(\mathbf{J}_s) & \mathbf{Z}_E^2(\mathbf{M}_s) \end{pmatrix}$$

- $\mathbf{Z}_E^1(\mathbf{J}_s)$ and $\mathbf{Z}_E^2(\mathbf{J}_s)$ are well-conditioned Submatrices.
- $\mathbf{Z}_E^1(\mathbf{M}_s)$ and $\mathbf{Z}_E^2(\mathbf{M}_s)$ are poorly-conditioned Submatrices.

Overall Result – An inaccurate solution



$a_n \times \text{RWG}$ Testing

$$\begin{pmatrix} \mathbf{Z}_E^1(\mathbf{J}_s) & \mathbf{Z}_E^1(\mathbf{M}_s) \\ \mathbf{Z}_E^2(\mathbf{J}_s) & \mathbf{Z}_E^2(\mathbf{M}_s) \end{pmatrix}$$

- $\mathbf{Z}_E^1(\mathbf{J}_s)$ and $\mathbf{Z}_E^2(\mathbf{J}_s)$ are poorly conditioned Submatrices.
- $\mathbf{Z}_E^1(\mathbf{M}_s)$ and $\mathbf{Z}_E^2(\mathbf{M}_s)$ are well-conditioned Submatrices.

Again, inaccurate Solution



RWG + a_n RWG Testing

- $Z_E^1(\mathbf{J}_s)$ and $Z_E^2(\mathbf{J}_s)$ are well conditioned Submatrices.
- $Z_E^1(\mathbf{M}_s)$ and $Z_E^2(\mathbf{M}_s)$ are well-conditioned Submatrices.

Or

- $Z_E^1(\mathbf{J}_s)$ and $Z_E^2(\mathbf{J}_s)$ are poorly-conditioned Submatrices.
- $Z_E^1(\mathbf{M}_s)$ and $Z_E^2(\mathbf{M}_s)$ are poorly-conditioned Submatrices.



-
- The Problem would be true for all other formulations – MFIE, CFIE, Muller formulations.
 - The Problem can happen for other situations – Apertures in a body and composite surfaces.
 - Far-fields may be acceptable with dense grids.
 - However, Near-fields are questionable.



Experimentation with Expansion Schemes

- Use Two separate functions to expand J_s and M_s .
- Preferably, these two functions should be spatially orthogonal to each other.
- Use same functions (or some approximations) for testing.



Method # 1

- Use RWG functions for \mathbf{J}_s .
- Use $\mathbf{a}_n \times \text{RWG}$ for \mathbf{M}_s .
- Use RWG functions for Testing.
- The EFIE Solution for this case is straightforward.

$$\left[j\omega \mathbf{A}_1 + \nabla \Phi_1 + \mathbf{a}_n \times \frac{\mathbf{M}_s}{2} + \nabla \times \mathbf{F}_1 \right]_{tan} = \mathbf{E}_{tan}^{inc}$$
$$\left[j\omega \mathbf{A}_2 + \nabla \Phi_2 - \mathbf{a}_n \times \frac{\mathbf{M}_s}{2} + \nabla \times \mathbf{F}_2 \right]_{tan} = 0$$

$$\begin{pmatrix} \mathbf{Z}_E^1(\mathbf{J}_s) & \mathbf{Z}_E^1(\mathbf{M}_s) \\ \mathbf{Z}_E^2(\mathbf{J}_s) & \mathbf{Z}_E^2(\mathbf{M}_s) \end{pmatrix}$$



- For MFIE Solution, one requires to compute the divergence of M_s .
- Use $a_n \times \text{RWG}$ functions for Testing.

$$\left[-\mathbf{a}_n \times \frac{\mathbf{J}}{2} - \nabla \times \mathbf{A}_1 + j\omega \mathbf{F}_1 + \nabla \Psi_1 \right]_{tan} = \mathbf{H}_{tan}^{inc}$$
$$\left[\mathbf{a}_n \times \frac{\mathbf{J}}{2} - \nabla \times \mathbf{A}_2 + j\omega \mathbf{F}_2 + \nabla \Psi_2 \right]_{tan} = 0$$



- Note that $a_n \times \text{RWG}$ functions have discontinuous derivatives.
- But can be handled in the following way.

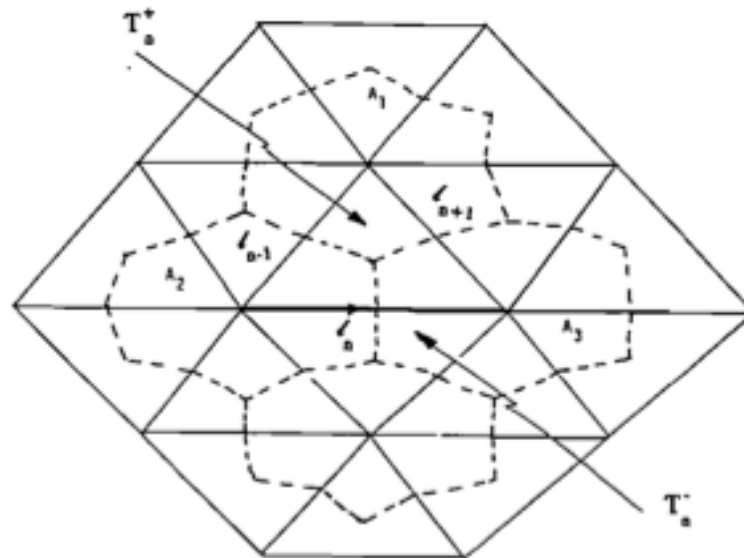


FIGURE 6. Magnetic charge patches associated with the n th edge.

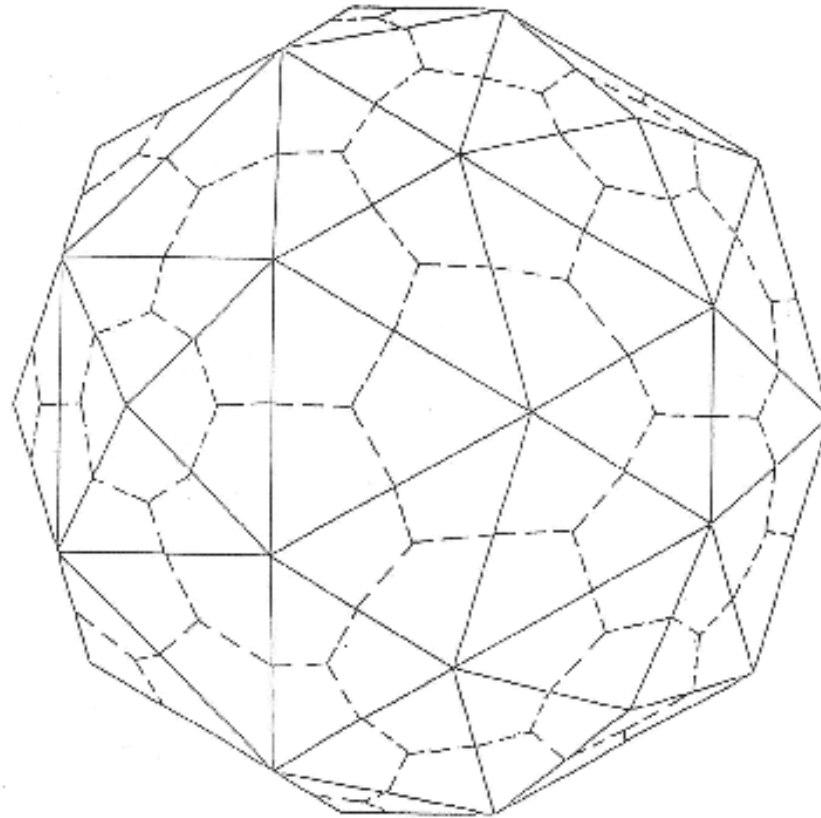


Another Scheme (Method #2)

- Use the conventional triangulation scheme RWG functions to expand the electric current J_s .
- Develop a dual grid and polygonal basis functions to expand M_s .



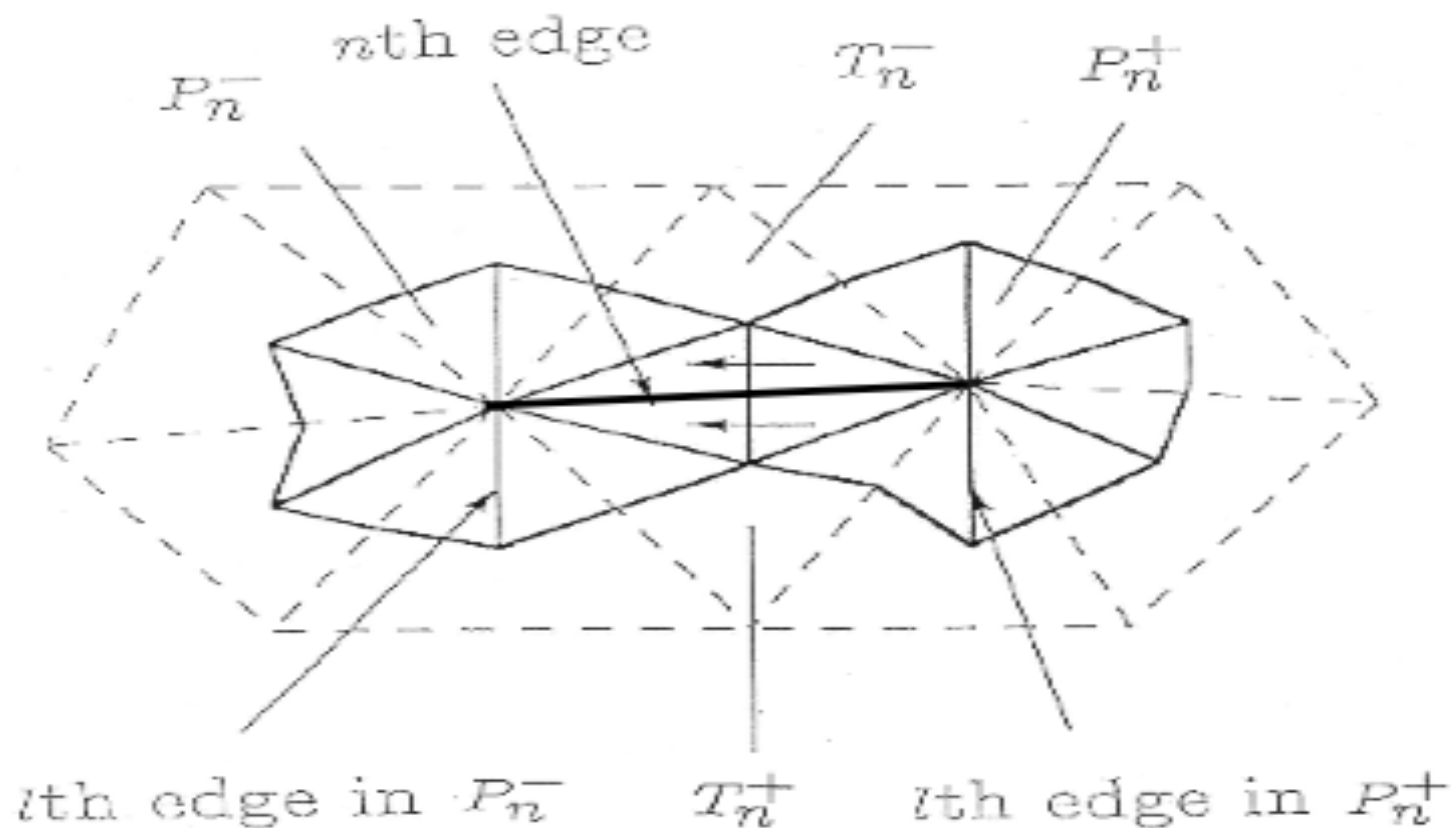
Dual Grid



A sphere surface modeled by triangular and corresponding polygonal patches.



Polynomial Basis Functions



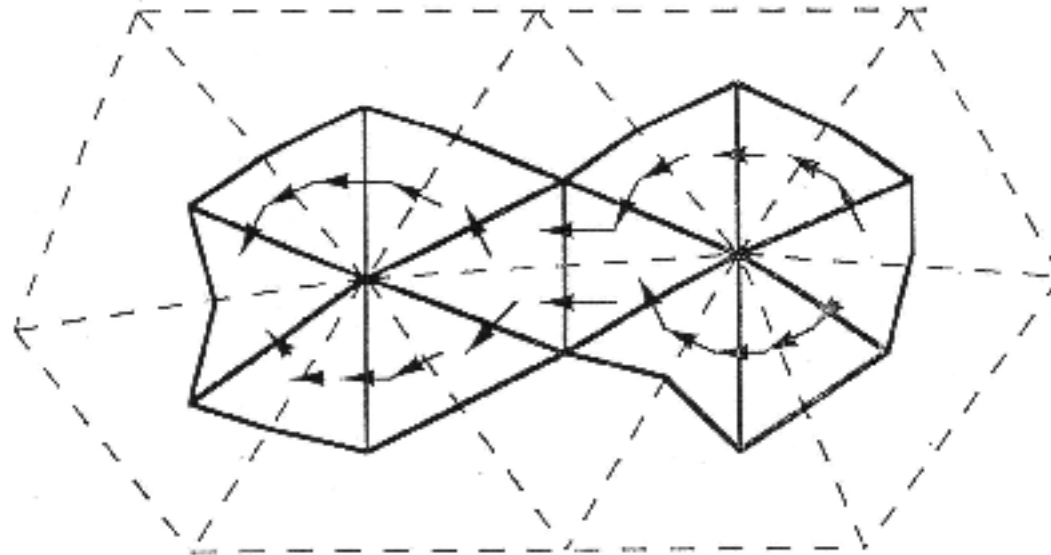


Mathematical Representation

$$\Lambda_n(\mathbf{r}) = \begin{cases} \sum_{l=0}^{L_n^\pm} C_{nl}^\pm \Lambda_{nl}^\pm(\mathbf{r}) & \text{for } \mathbf{r} \in P_n^\pm \\ 0 & \text{otherwise} \end{cases}$$



Current flowing in the Polygon Pair





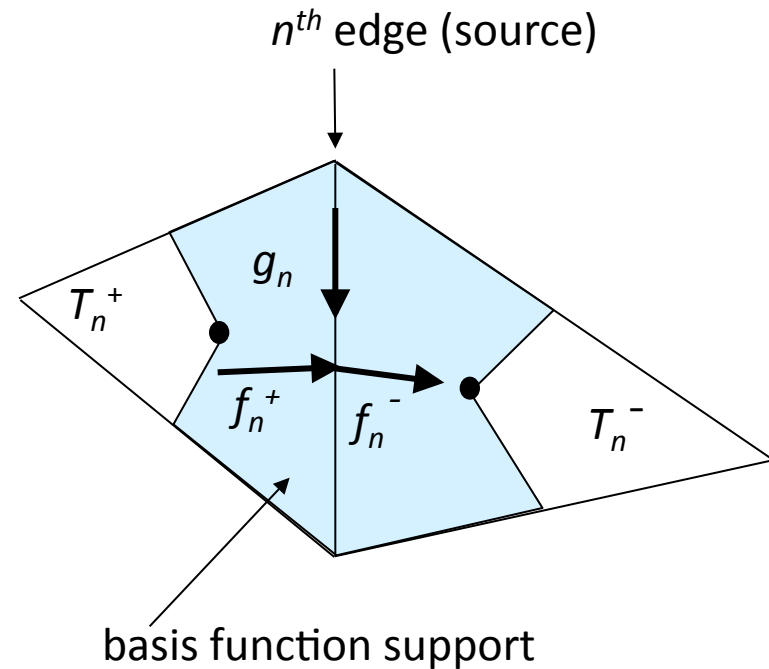
Yet Another Scheme (Method # 3)

Pulse-Like Functions on Triangle Pair

$$\hat{\mathbf{n}} \times \mathbf{g}_n = \mathbf{f}_n$$

$\hat{\mathbf{n}}$ = outward unit normal

$$|\mathbf{f}_n^+| = |\mathbf{f}_n^-| = |\mathbf{g}_n| = 1$$



$$\mathbf{J}_n = I_n (\mathbf{f}_n^+ + \mathbf{f}_n^-)$$

$$\mathbf{M}_n = I_{N+n} \mathbf{g}_n$$



Charge Patches for \mathbf{J}

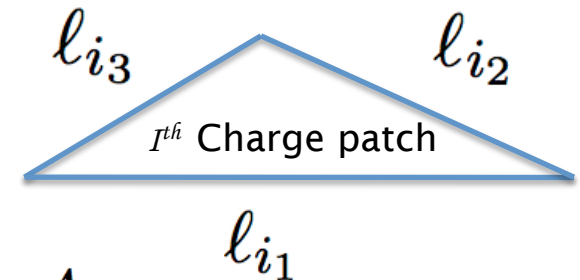
Let N_p be the total number of triangles, and let

$$q_s = \sum_{i=1}^{N_p} \alpha_i P_i \quad \text{Where } P_i(\mathbf{r}) = \begin{cases} 1, & \mathbf{r} \in T_i \\ 0, & \text{otherwise} \end{cases}$$

$$\int_{T_i} q_s ds = \int_{T_i} \frac{\nabla_s \bullet \mathbf{J}}{-j\omega} ds$$

$$= \frac{j}{\omega} \oint_{C_i} \mathbf{J} \bullet d\mathbf{l}$$

$$= \frac{j}{\omega} [I_{i1} l_{i1} + I_{i2} l_{i2} + I_{i3} l_{i3}] = \alpha_i A_i$$



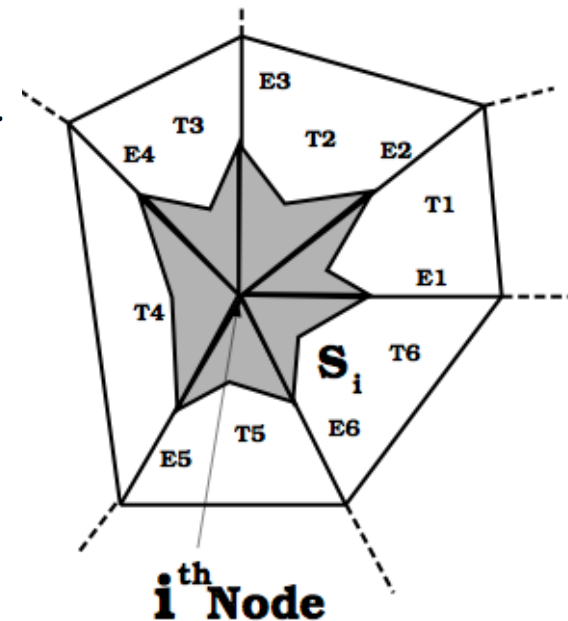
$$\alpha_i = \frac{j}{\omega} \left[\frac{I_{i1} l_{i1} + I_{i2} l_{i2} + I_{i3} l_{i3}}{A_i} \right]$$



Charge Patches for M

Let $q_S = \sum_{i=1}^{N_n} \alpha_i P_i$ $P_i(\mathbf{r}) = \begin{cases} 1, & \mathbf{r} \in S_i \\ 0, & \text{otherwise.} \end{cases}$

$$\begin{aligned} \int_{S_i} q_S dS &= \int_{S_i} \frac{\nabla_s \cdot \mathbf{J}}{-j\omega} dS \\ &= \frac{j}{\omega} \oint_{C_i} \mathbf{J} \cdot \mathbf{n}_\ell dl \\ &= \frac{j}{\omega} \sum_{j=1}^{E_K} I_{ij} [\boldsymbol{\ell}_{ij} \cdot (\mathbf{r}_{ij}^{c+} \times \mathbf{n}_{ij}^+ + (\mathbf{r}_{ij}^{c-} \times \mathbf{n}_{ij}^-))] \end{aligned}$$



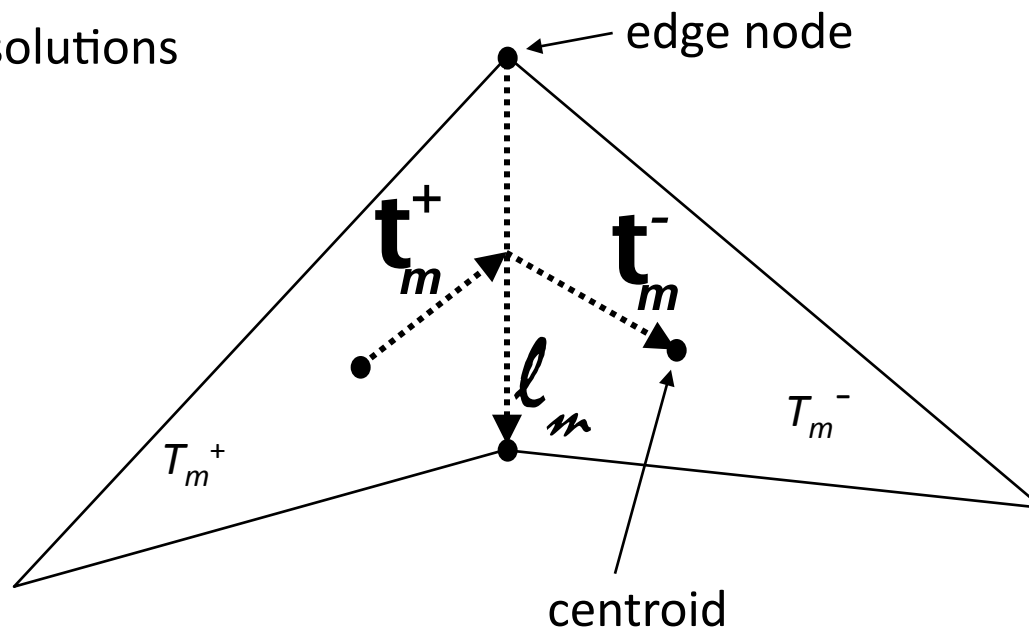
$$\alpha_i = \frac{j}{\omega A_{S_i}} \sum_{j=1}^{E_K} I_{ij} [\boldsymbol{\ell}_{ij} \cdot (\mathbf{r}_{ij}^{c+} \times \mathbf{n}_{ij}^+ + (\mathbf{r}_{ij}^{c-} \times \mathbf{n}_{ij}^-))]$$



Testing Vectors

\mathbf{t}_m^+ , \mathbf{t}_m^- : EFIE solutions

l_m : HFIE solutions

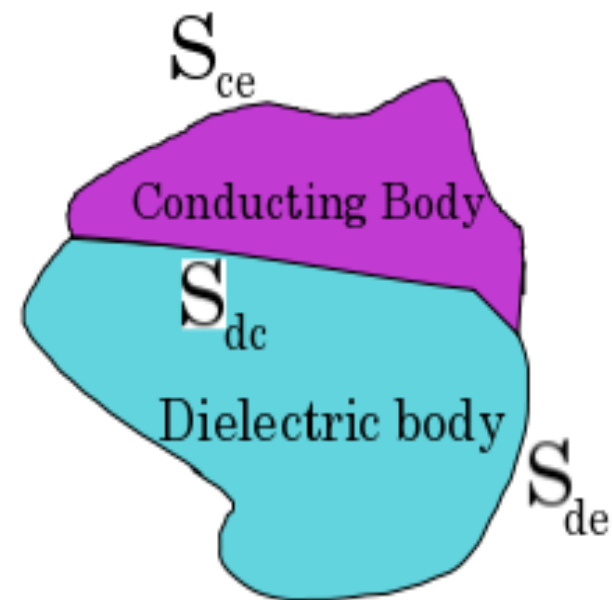




An Alternate Formulation

- Consider the following Composite Body Problem

- On surface S_{ce} ----- Only J_{ce} .
- On surface S_{de} ----- J_{de} and M_{de} .
- On surface S_{dc} -----Only J_{dc} .
- Use PMCHWT Formulation.



- OK for far-field calculations.
- For near-field quantities, extra work is needed to obtain physical currents from equivalent currents.



Some Observations

- Dielectric Body Problem is more complicated than PEC problem.
- If RWG functions are used for expansion and testing, one must be very careful while applying the numerical procedures.
- Ideally, it is recommended to use two spatially orthogonal functions in the numerical scheme.
- It is possible to get acceptable far-field quantities using only RWG functions.
- While using software packages, one needs to know how the dielectric materials are treated.



Water meter antenna



Radiating Element



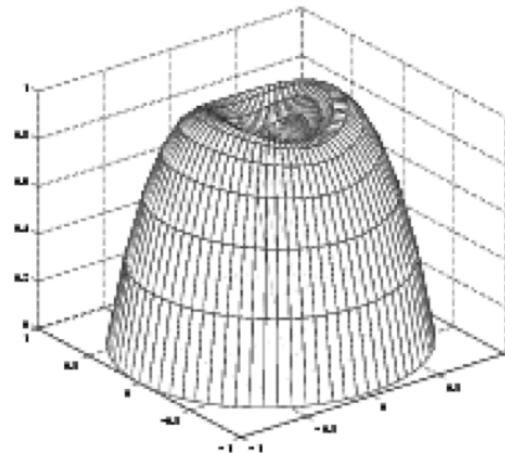
(a)

Feed



(b)

Insulator



Radiation Pattern



Time Domain Problems

- Here we solve the scattering problem directly in time-domain – Useful for Impulse radar, Wideband solutions, and signature studies.
- No matrix inversion – solution is obtained iteratively.

Time Domain Electromagnetics
Academic Press, 2001



Consider the following problem:

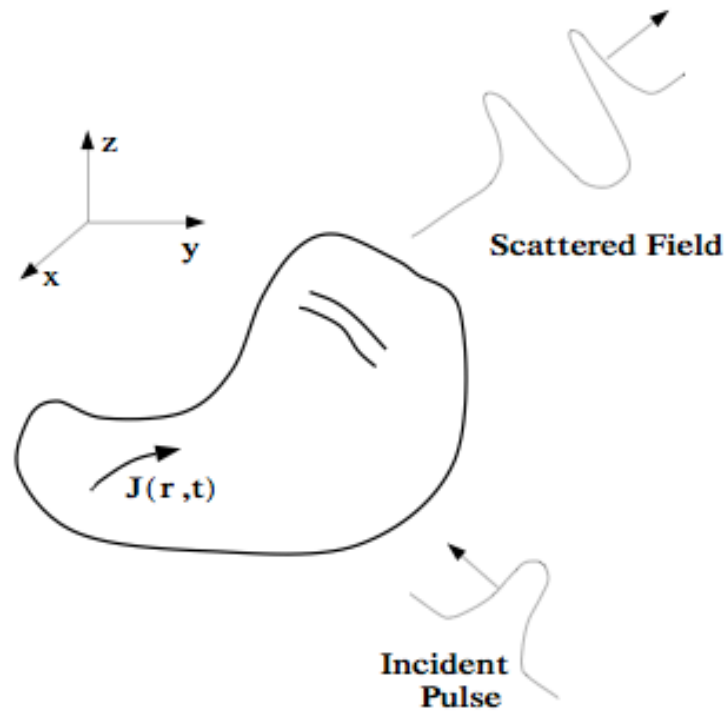


Figure 1: Transient pulse incident upon an arbitrarily shaped body.

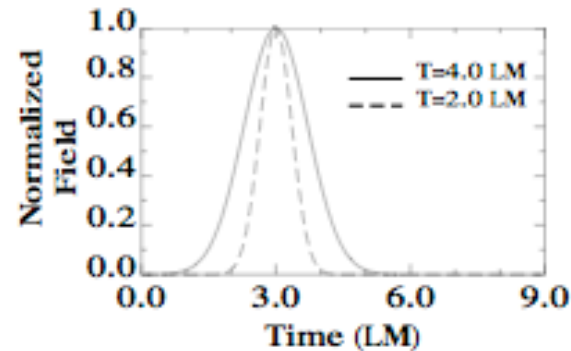


Direct Time Domain Solutions are better suited to:

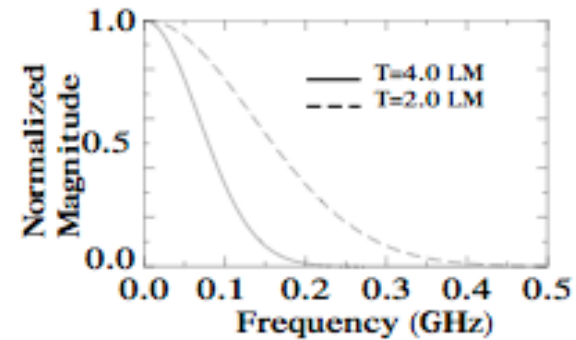
- Short-pulse radar systems.
- EMP studies.
- Provide better visualization.
- Provides opportunity to observe and interpret scattering behavior.
- Provides broadband information.



Incident Field



(a)



(b)

$$\mathbf{E}^i(\mathbf{r}, t) = \mathbf{E}_o \frac{4}{T\sqrt{\pi}} e^{-\gamma^2}$$

where

$$\gamma = \frac{4}{T}(ct - ct_o - \mathbf{r} \cdot \mathbf{a}_k),$$



Time Domain EFIE

$$\left[\frac{\partial \mathbf{A}(\mathbf{r}, t)}{\partial t} + \nabla \Phi(\mathbf{r}, t) \right]_{tan} = \mathbf{E}_{tan}^i(\mathbf{r}, t)$$

where

$$\mathbf{A}(\mathbf{r}, t) = \mu \int_S \frac{\mathbf{J}(\mathbf{r}', t - \frac{R}{c})}{4\pi R} dS' ,$$

$$\Phi(\mathbf{r}, t) = \frac{1}{\epsilon} \int_S \frac{q_s(\mathbf{r}', t - \frac{R}{c})}{4\pi R} dS' ,$$



Final Equation

$$\begin{aligned} & [\kappa_{mm} \cdot \frac{l_m}{2} (\rho_m^{c+} + \rho_m^{c-})] I_m(t_j) = \\ & \frac{l_m}{2} (\rho_m^{c+} + \rho_m^{c-}) \cdot (\Delta t) \mathbf{E}^i(\mathbf{r}_m, t_{j-1}) \\ & - \frac{l_m}{2} (\rho_m^{c+} + \rho_m^{c-}) \cdot [\mathbf{A}'(\mathbf{r}_m, t_j) - \mathbf{A}(\mathbf{r}_m, t_{j-1})] \\ & + l_m(\Delta t)[\Phi(\mathbf{r}_m^{c+}, t_{j-1}) - \Phi(\mathbf{r}_m^{c-}, t_{j-1})]. \end{aligned}$$

Lastly, we can write Eq. (44) in matrix form as

$$[\boldsymbol{\alpha}][\mathbf{I}(t_j)] = [\mathbf{F}(t_j)] + [\boldsymbol{\beta}][\mathbf{I}(t_R)].$$



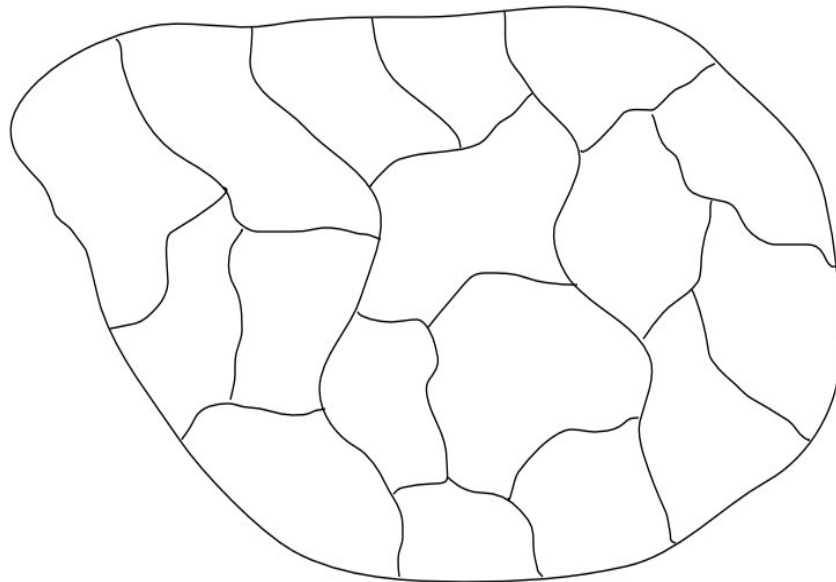
Conclusions

- RWG functions have been used for a variety of problems in numerical electromagnetic problems.
- Also used in other areas – Acoustic scattering.
- New improvements include: developing faster solutions (FMM), adaptive basis functions to generate sparse moment matrix (Killian and Rao, IEEE Transactions on A&P, 2011), Domain Decomposition to handle large problems, and Adaptive Cross Approximation (Mercury MoM).



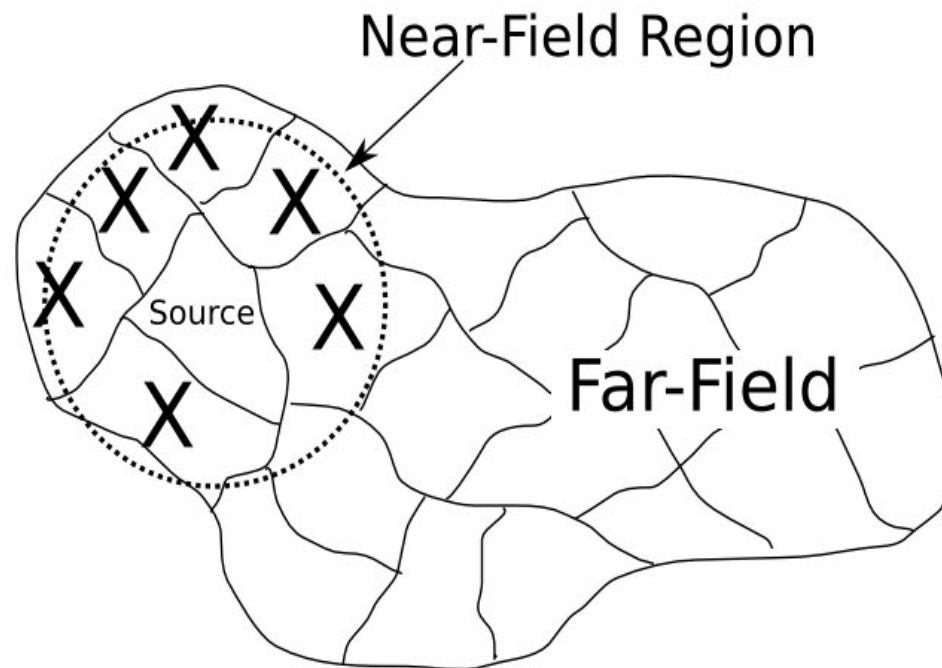
New domain Decomposition Method

- Domain Decomposition – Disjoint groups of sub-domain functions
- Functions in a group are geometrically close to one another
- Each function belongs to one and only one group.



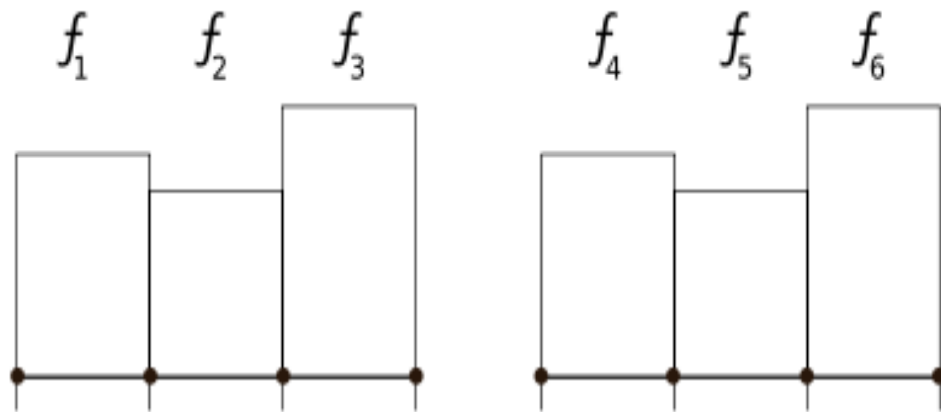


- Decouple a given group from other groups- Can be accomplished by generating new set of basis functions.
- It is possible to solve each group separately and obtain the total solution.





Example – Two 2D strips





$$Z = \left[\begin{array}{c} \left[\begin{array}{ccc} Z_{1,1} & Z_{1,2} & Z_{1,3} \\ Z_{2,1} & Z_{2,2} & Z_{2,3} \\ Z_{3,1} & Z_{3,2} & Z_{3,3} \\ Z_{4,1} & Z_{4,2} & Z_{4,3} \\ Z_{5,1} & Z_{5,2} & Z_{5,3} \\ Z_{6,1} & Z_{6,2} & Z_{6,3} \end{array} \right] \\ \left[\begin{array}{ccc} Z_{1,4} & Z_{1,5} & Z_{1,6} \\ Z_{2,4} & Z_{2,5} & Z_{2,6} \\ Z_{3,4} & Z_{3,5} & Z_{3,6} \\ Z_{4,4} & Z_{4,5} & Z_{4,6} \\ Z_{5,4} & Z_{5,5} & Z_{5,6} \\ Z_{6,4} & Z_{6,5} & Z_{6,6} \end{array} \right] \end{array} \right]$$

$$= \left[\begin{array}{cc} [Z_{G_1 G_1}] & [Z_{G_1 G_2}] \\ [Z_{G_2 G_1}] & [Z_{G_2 G_2}] \end{array} \right]$$

New basis function:

$$g_1 = f_1 + \alpha_1 f_4 + \beta_1 f_5 + \gamma_1 f_6$$

$$g_2 = f_2 + \alpha_2 f_4 + \beta_2 f_5 + \gamma_2 f_6$$

$$g_3 = f_3 + \alpha_3 f_4 + \beta_3 f_5 + \gamma_3 f_6$$

Criteria (g_1) :

$$Z_{4,1} + \alpha_1 Z_{4,4} + \beta_1 Z_{4,5} + \gamma_1 Z_{4,6} = 0$$

$$Z_{5,1} + \alpha_1 Z_{5,4} + \beta_1 Z_{5,5} + \gamma_1 Z_{5,6} = 0$$

$$Z_{6,1} + \alpha_1 Z_{6,4} + \beta_1 Z_{6,5} + \gamma_1 Z_{6,6} = 0$$



$$\begin{bmatrix} \alpha_1 \\ \beta_1 \\ \gamma_1 \end{bmatrix} = - \begin{bmatrix} Z_{4,4} & Z_{4,5} & Z_{4,6} \\ Z_{5,4} & Z_{5,5} & Z_{5,6} \\ Z_{6,4} & Z_{6,5} & Z_{6,6} \end{bmatrix}^{-1} \begin{bmatrix} Z_{4,1} \\ Z_{5,1} \\ Z_{6,1} \end{bmatrix}$$

Solve for weights

$$\tilde{Z}_{2,1} = Z_{2,1} + \alpha_1 Z_{2,4} + \beta_1 Z_{2,5} + \gamma_1 Z_{2,6}$$

Create new matrix

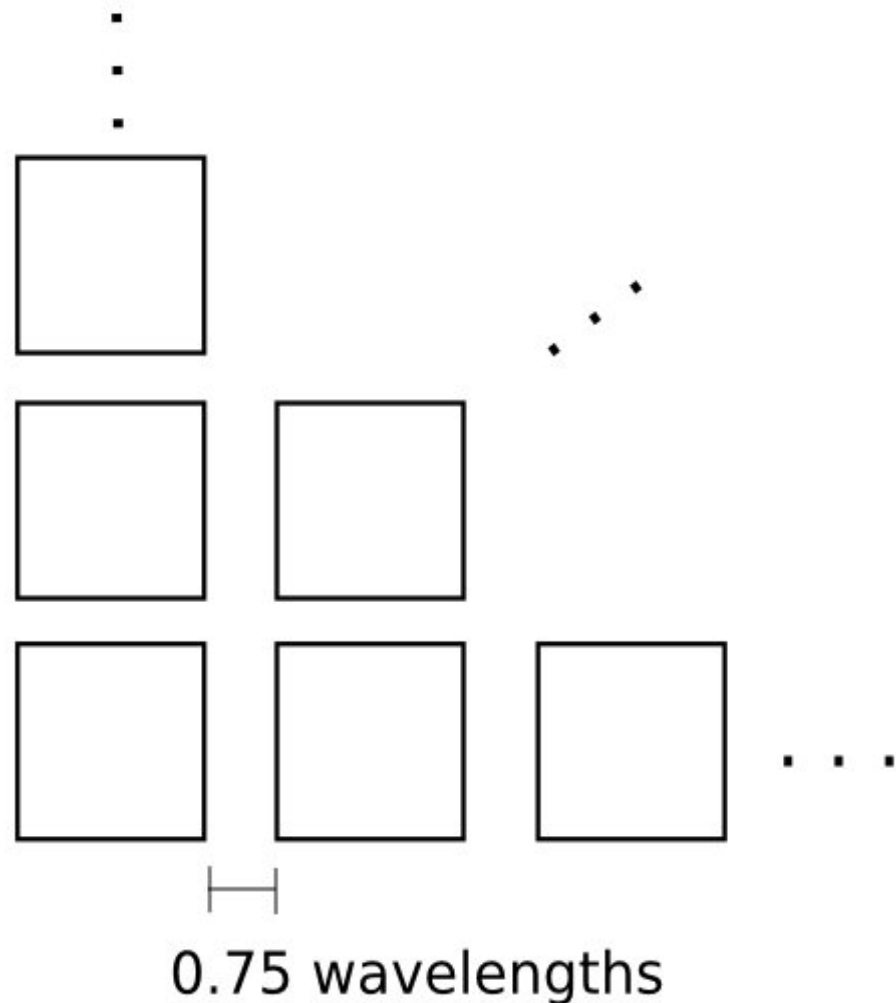
$$\tilde{Z} = \begin{bmatrix} \tilde{Z}_{G_1 G_1} & 0 \\ 0 & \tilde{Z}_{G_2 G_2} \end{bmatrix}$$

$$R = \begin{bmatrix} 1 & 0 & 0 & \alpha_4 & \alpha_5 & \alpha_6 \\ 0 & 1 & 0 & \beta_4 & \beta_5 & \beta_6 \\ 0 & 0 & 1 & \gamma_4 & \gamma_5 & \gamma_6 \\ \alpha_1 & \alpha_2 & \alpha_3 & 1 & 0 & 0 \\ \beta_1 & \beta_2 & \beta_3 & 0 & 1 & 0 \\ \gamma_1 & \gamma_2 & \gamma_3 & 0 & 0 & 1 \end{bmatrix}$$



3D Results - Finite Planar Array

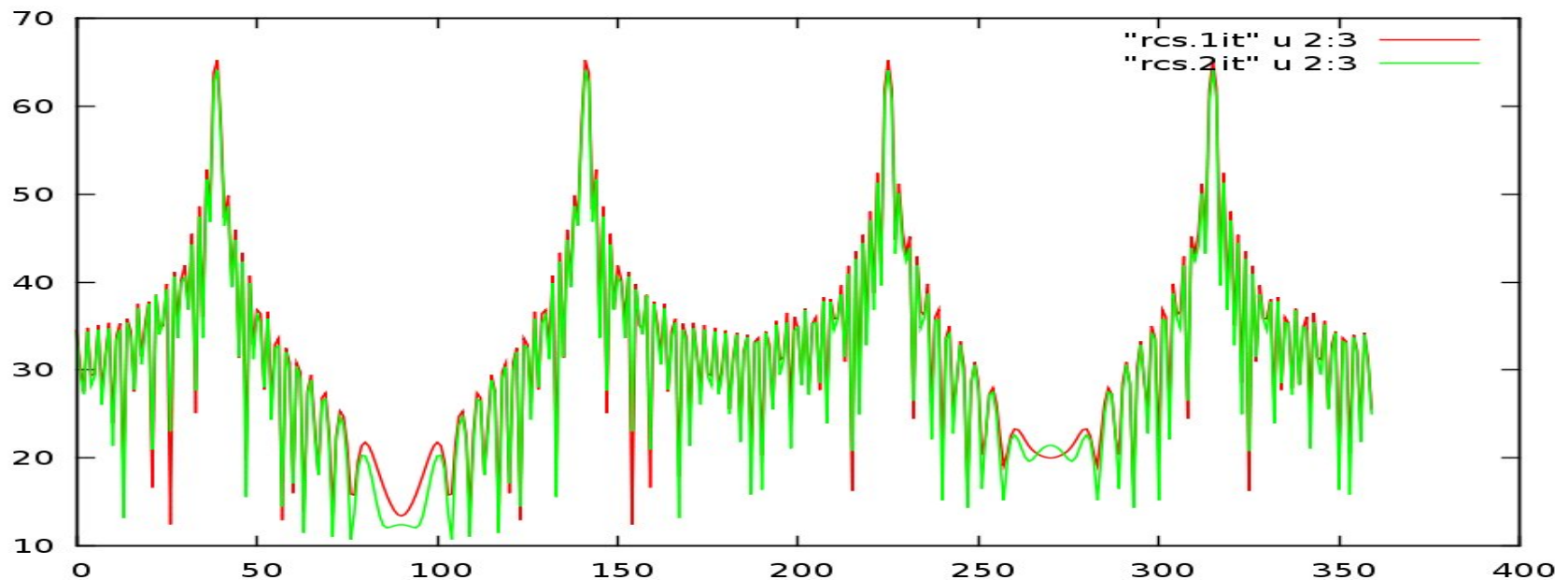
- Finite Periodic Array
- EFIE
- 50 x 50 grid of
0.5 lambda x 0.5 lambda plates
- 64 unknowns per plate
- 0.75 lambda spacing
- 160,000 total unknowns
- Null fields produced
on adjacent plates
- Redundant coefficients
- $E_{\theta} = 120\pi$; $E_{\phi} = 0$
- $\Theta = 45 \text{ deg}$ $\Phi = 0 \text{ deg}$





3D Results - Planar Array

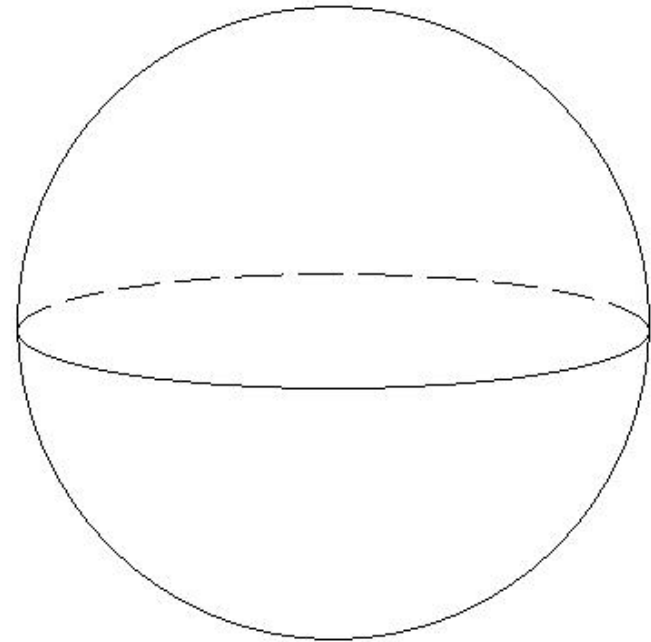
- 1 iteration = 0.288 average error per term
- 2 iterations = 0.122 average error per term
- ~19.5 hours wall clock time with 8 CPUs (includes time for RCS calculation on single CPU)
- Matrix approximations can be used for speedup





3D Results - Sphere

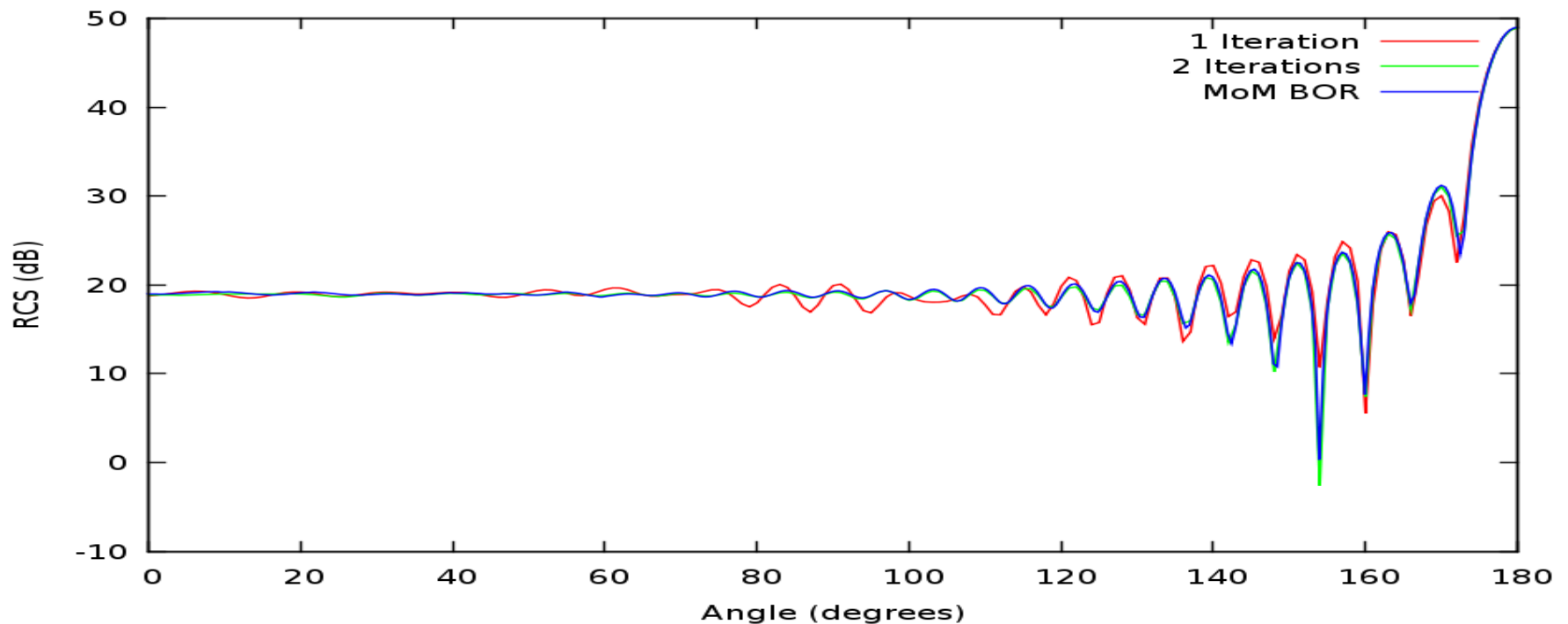
- 5 lambda radius
- CFIE
- 92550 unknowns
- 314 Groups – each roughly 1 lambda² in surface area
- Null fields produced on groups within 2 lambda radius (typically around 3000 points)
- ~ 2.5 GB storage
- $E_{th} = 120\pi$; $E_{phi} = 0$
- $\Theta = 45 \text{ deg}$ $\Phi = 0 \text{ deg}$





3D Results - Sphere

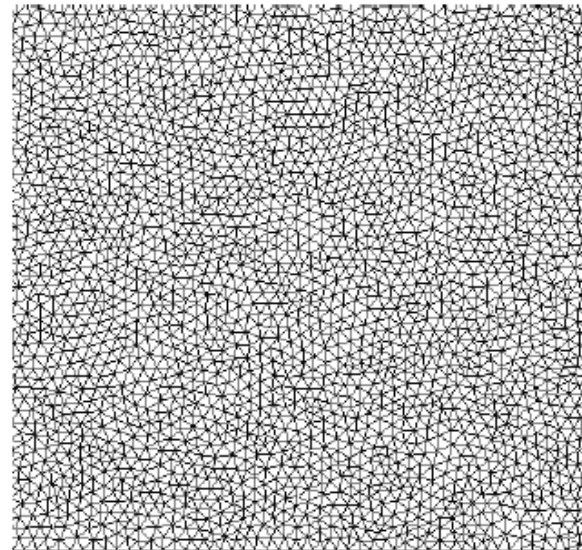
- 1 iteration = 0.096 average error per term
- 2 iterations = 0.014 average error per term
- ~26 hours wall clock time with 8 CPUs (includes time for RCS calculation on single CPU)
- Matrix approximations can be used for speedup





3D Results - Square Plate

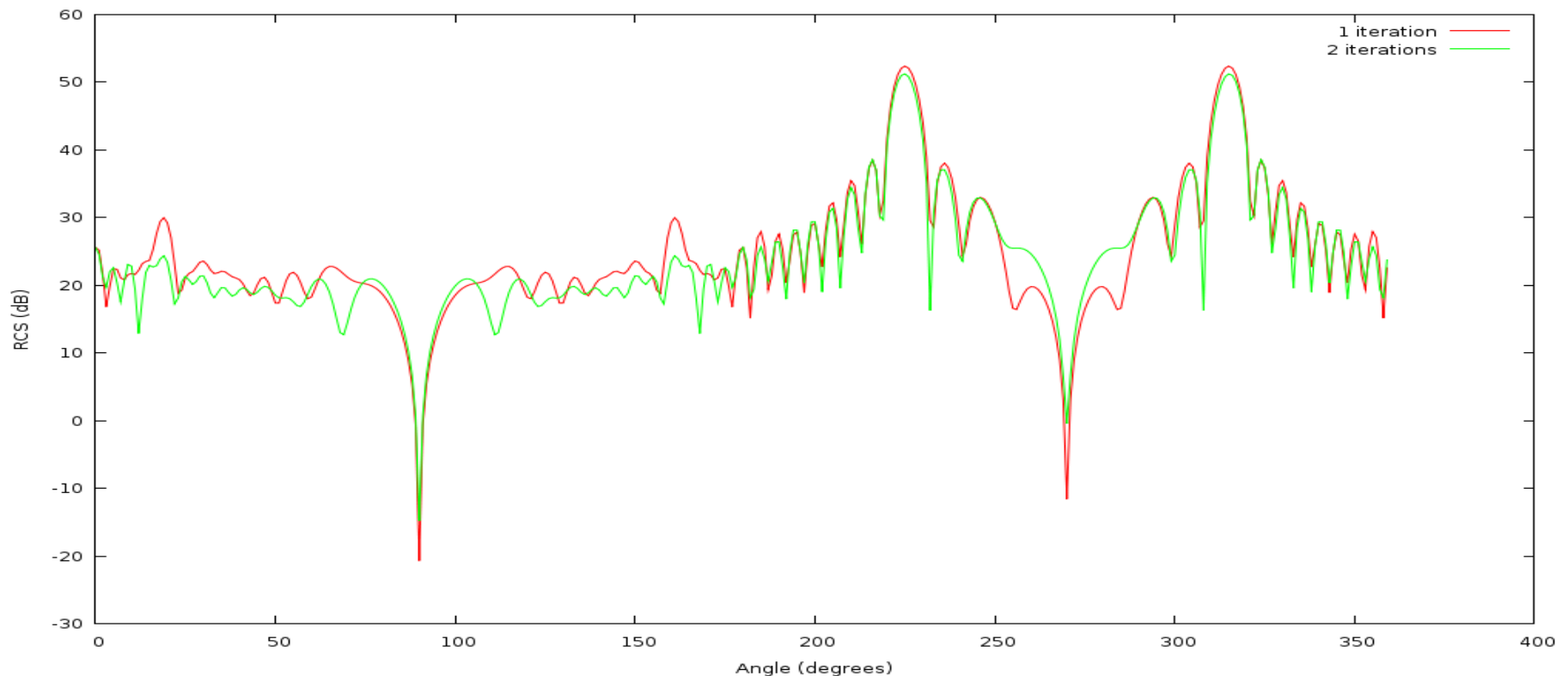
- $12 \lambda \times 12 \lambda$ square plate
- EFIE
- 42883 unknowns
- 144 Groups – each roughly $1 \lambda^2$ in surface area
- Null fields produced on groups within 2 lambda radius (typically around 2800 points)
- ~ 185 MB storage
- $E_{\theta} = 120\pi$; $E_{\phi} = 0$
- $\Theta = 45 \text{ deg}$ $\Phi = 0 \text{ deg}$





3D Results - Square Plate

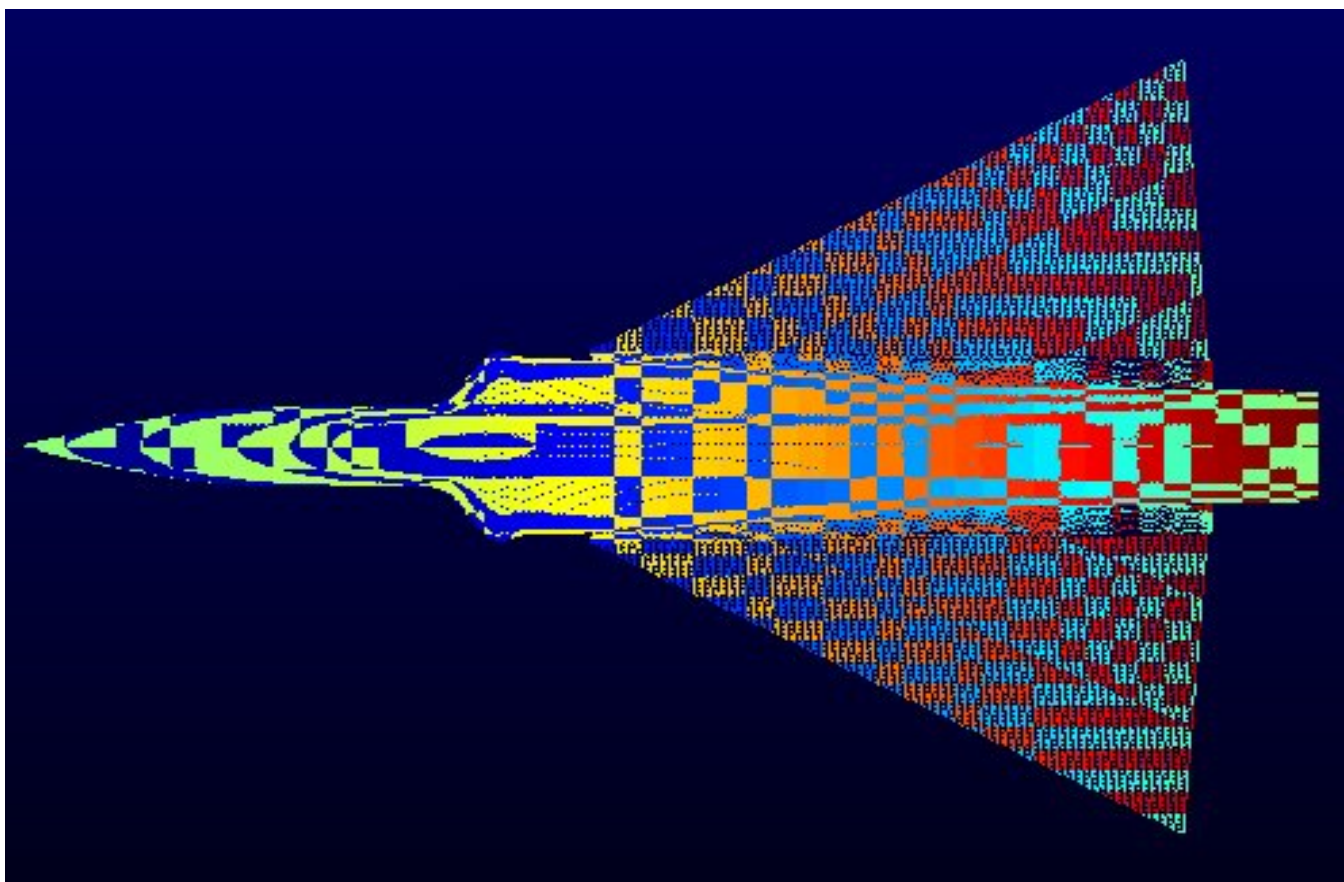
- 1 iteration = 0.612 average error per term
- 2 iterations = 0.232 average error per term
- ~ 2 hours 45 mins wall clock time with 8 CPUs
(includes time for RCS calculation on single CPU)





3D Results - Aircraft

- French Mirage
- ~ 160,000 unknowns
- Patches represent groups.





3D Results - Aircraft

- 1 iteration = 0.224 average error per term
- 2 iterations = 0.218 average error per term
- ~ 5 days 7 hours wall clock time with 8 CPUs
(includes time for RCS calculation on single CPU)

